

Archaeometallurgy of ferrous artefacts of the Patriótica Iron Factory (XIX century, Ouro Preto, Brazil)

<http://dx.doi.org/10.1590/0370-44672021740019>

Fernando José Gomes Landgraf^{1,5}

<https://orcid.org/0000-0001-5390-0879>

Matheus Yuri Quisbert Ribeiro^{2,6}

<https://orcid.org/0000-0002-4830-5060>

Guilherme Inácio Lima da Rosa^{2,7}

<https://orcid.org/0000-0003-2246-8168>

Paulo Sérgio Germano Carvalho^{3,8}

<https://orcid.org/0000-0002-7053-3107>

Daniel Luiz Rodrigues^{1,9}

<https://orcid.org/0000-0003-1380-4844>

Rafael Rocha Maia^{1,4,10}

<https://orcid.org/0000-0002-6935-5032>

Flávio Beneduce Neto^{1,11}

<https://orcid.org/0000-0001-6447-7404>

Cesar Roberto Farias Azevedo^{1,12}

<https://orcid.org/0000-0002-0813-6231>

¹Universidade de São Paulo – USP, Escola Politécnica – EP, Departamento de Engenharia Metalúrgica e de Materiais, São Paulo – São Paulo – Brasil.

²Universidade de Mogi das Cruzes - UMC, Departamento de Engenharia. Mecânica, São Paulo - São Paulo – Brasil.

³Pontifícia Universidade Católica de São Paulo - PUC-SP, Departamento de Engenharia Civil, São Paulo - São Paulo – Brasil.

⁴Faculdade de Tecnologia de São Paulo – Fatec, Departamento de Engenharia de Produção, São Paulo - São Paulo - Brasil.

E-mails: ⁵f.landgraf@usp.br,

⁶m.yuriquisbert@gmail.com,

⁷guilherme.inacio@hotmail.com, ⁸pscarvalho@pucsp.br,

⁹danieljunior@usp.br, ¹⁰rafael.maia@alumni.usp.br,

¹¹beneduce@usp.br, ¹²c.azevedo@usp.br

Abstract

The article reviews the metallurgical processes used in the first industrial iron-works operated in Brazil, the Patriótica Iron Factory, from 1812 to 1831. It discusses its impact on the ironmaking plants that spread in Minas Gerais's state during the XIX century. The remnants of this Factory in Ouro Preto were the first industrial site listed by the Brazilian Historic Heritage Authority (SPHAN) in 1938. Vale SA, owner of the site, and the National Historic and Artistic Heritage Institute (IPHAN) authorised collecting samples from two ferrous artefacts found in the old Factory, a hammer and an eyebolt nailed to the remnants of one of the reduction furnaces. The eyebolt's microstructure suggests that this part was produced in the *Patriótica* Iron Factory, while the hammer's microstructure indicates that this component was not produced in the *Patriótica* Iron Factory.

Keywords: history of Brazilian ironmaking; The Patriótica Iron Factory; archaeometallurgy; direct reduction; slag inclusion; microstructure; provenance.

1. Introduction

This article addresses the history of the *Fábrica Patriótica* and investigates the relationship between the slag inclusions' microstructure of two ferrous objects collected in the remnants of the *Fábrica* and the smelting and forging processes used at the beginning of the XIX century. To begin with, some words about the name of the place. Before 1800, the Brazilian ironworks was called "Engenho de Ferro", Iron Mill. At the beginning of the XIX century, a new name was used, "Fábrica", Factory. At the end of the XIX century, another change: the word "Usina", siderurgy, like the *Usina Esperança* in Itabirito, 1890. In this article, we will use *Factory*. The *Patriótica* Iron Factory was designed and managed by the German engineer, Baron von Eschwege. The iron plant, located in Ouro Preto (Minas Gerais state, Brazil), started operation in 1812 and was the first Factory to industrially produce iron in Brazil (Rogers, 1962; Eschwege, 1979; Pinho and Neiva, 2012). The *Patriótica* Iron Factory was the first industrial site listed by the Brazilian Historic Heritage Authority in 1938 (IPHAN, 2021; Dezen-Kempton, 2011; Rodrigues, 2012). Its archaeological site, well kept by Vale S.A., contains numerous ferrous objects and four

iron-production furnaces, useful to improve the understanding of ironmaking history in Brazil (see Figures 1-a to 1-c and Figure 2). The iron smelting processes at that time could be classified into two major classes. The direct reduction process produces iron in solid-state, without forming a liquid iron phase, using charcoal and carbon monoxide as reductant agents (Miller, 1976). The batches of iron ore (hematite, limonite, or magnetite) and coal in the furnace are transformed by a discontinuous process into a "ferrous product" or a pasty mass of sponge iron, as described by H. C. and L. H. Hoover (Agricola, 2011):

"The first method (the direct reduction of malleable iron from ore) is that of primitive iron-workers of all times and all races and requires little comment. A pasty mass was produced, which was subsequently hammered to make it exude the slag, the hammered mass being the ancient "bloom."

With the evolution of the direct reduction process, the furnaces became larger and higher. The air blow's flux was increased, resulting in higher iron production and lower fuel consumption as the gases moving upward from the

hot region preheated and pre-reduced the ore (Miller, 1976). The furnace's height could vary from half a meter to three meters, while the furnace's interior space featured a square or circular cross-section, the latter with a diameter smaller than one meter. The profile of this inner space was, in general, a cone or pyramidal shaft, which could be wider at the top or bottom. In most cases, the bloom was retrieved from a bottom opening. One exception is the Catalan forge, where the bloom was extracted by the broader top of that furnace type (Percy, 1864). The air could be blown into the reduction furnace by natural draft. Still, higher productivity was obtained by hand or water-powered bellows, water trompes, and steam engines (introduced in England in the early XIX century) (Ågren, 1998).

The increase in the temperature also increased the solubility of carbon in the produced solid iron, gradually reducing its melting point from 1540°C to 1150°C, leading to the formation of a high-carbon liquid iron, also called pig iron, and the development of the blast furnaces and the indirect reduction process (Miller, 1976).

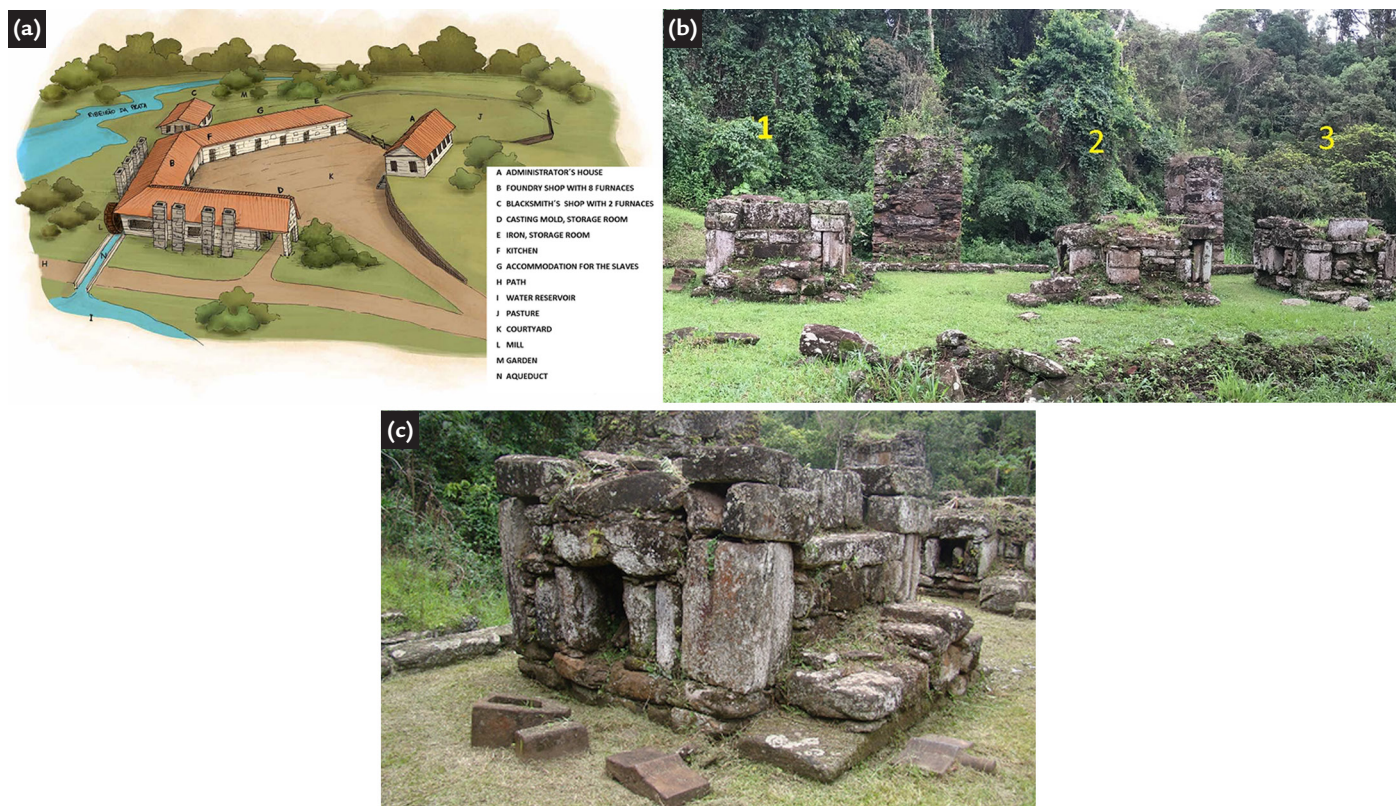


Figure 1 - (a) Scheme showing the *Patriótica* Iron Factory, adapted from

(Pinho and Neiva, 2012); (b) Four reduction furnaces at the *Patriótica* Iron Factory, section B. In the relic of

furnace n° 2, there were two reduction furnaces. On the left side of the furnace's remnant of the furnace n° 1, four heavy pieces of iron were found on the floor. The eyebolt segment was removed from the relic of the furnace n° 3; (c) Photo showing the furnace's exit.

The indirect reduction process of iron ores appeared in China in 500BC and Europe around 1,400 AD (Tylecote, 1984) and took place in two steps: first adding carbon into the process and producing the pig iron; and, in a second step, removing the excess carbon from the pig iron to make steel (Jockenhövel and Willms, 1997). In

1.1 Historical background in Brazil

There are reports of the existence of "*engenhos de ferro*" in colonial Brazil since the 16th century (currently in the region of the state São Paulo) (Landgraf et al., 1994). Despite the demand for iron tools in the mining province of Minas Gerais in the 18th century, the authors could not find any documents confirming local iron production in that period. In 1780, the governor of Minas Gerais sent a document to the Portuguese government describing the problematic situation in the province (caused by a decrease in the production of gold) and recommending the installation of an iron factory as a counter-measure to facilitate the digging of mines (Menezes, 1897). The "*Alvará de Proibição de Fábricas e Manufaturas*" (Manufacture and Fabric Prohibition Law) was issued in 1785 by the Queen of Portugal, Maria I, prohibiting factories and manufacturers of gold, silver, and textiles in Brazil. This law ban has often been mentioned as an impediment to iron production in Brazil in the late 18th century (Felicíssimo, 1969). Still, this law did not state any prohibition on the manufacture of iron products. The criminal proceedings of the "*Inconfidência Mineira*" (a Brazilian independence movement known as The Minas Conspiracy of 1789) did not list any "iron entrepreneur" among the collaborators of the Brazilian liberation movement. One of its leaders, Mr Maciel, studied chemistry and mineralogy in Coimbra and lived in 1786 in Birmingham, England, the world capital

1.2 Technological aspects of the Patriótica Iron Factory

The Portuguese government hired the German Baron Wilhelm Ludwig von Eschwege to help implement the ironmaking industry in Portugal and Brazil. He arrived in Rio de Janeiro in 1810 and became head of the Royal Office of Mineralogy before being nominated Intendant of the Gold Mines. He convinced the governor of Minas Gerais to participate in the financing of an iron factory (Baeta, 1973), which was conceived to produce 15 tons of malleable iron per year (50 kg per day) to meet

the early XIX century in Europe, most of the iron was produced by blast furnaces (capacity of one ton of pig iron per day). Pig iron was also extensively used in the manufacture of parts by solidifying sand moulds (cast-iron). The fabrication of malleable iron bars from pig iron was more economical than the direct reduction, but

of iron, as well as the Boulton and Watt steam engines at that time. Maciel told the other "*inconfidentes*" (independence revolutionaries) that it would be easy to start the iron production after the establishment of the new republic (Araújo and Filgueiras, 2017). His comment reinforces that there was no commercial iron production in the province of Minas Gerais. In 1795, a law was issued encouraging the local production of iron (Vidal and Luca, 2014), which finally "started" in Minas Gerais in the early XIX century, using the direct reduction process. In 1833, Eschwege (1979) suggested that the reduction process of one of the first small iron mills in Minas Gerais's province had an African origin:

"In Minas Gerais's province, the manufacture of iron became known at the beginning of this century through African slaves. The iron was first manufactured in Antonio Pereira (now a district of Ouro Preto) by a slave of Captain Antonio Alves."

It is a fact that there was already iron production in southern Africa in the second millennium AD (Miller, 2002). Small reduction furnaces, which produced less than 10 kg of iron per batch, were also used in Portugal (Custodio, 2002). Eschwege (1979) wrote, "*Some blacksmiths and farmers made some iron in blacksmith's forges and even in small furnaces*". He called these furnaces as *Eisenschmelz-Oefchen*, which was translated as "forninhos", little furnaces. In Brazil, the blacksmith's work was

it was much more difficult. The pig iron had to solidify before being reheated in refining furnaces, where the carbon content of the iron was lowered by its oxidation using air blowing. The iron had to be forged at high temperatures to expel the excess slag inclusions trapped in the metal after the refining stage (Miller, 1976).

in the hands of the African slaves, and these blacksmith tents, which formed and shaped the imported iron bars, were commonly found in the province of Minas Gerais (Alfagali, 2012). There is no evidence yet to confirm the hypothesis that the technique of producing iron from ore using small reduction furnaces in the province Minas Gerais was imported from Africa.

The creation of The Patriótica Iron Factory in Brazil in 1811 was part of the ironmaking program of the Portuguese government, encouraged by Minister Rodrigo de Souza Coutinho (Varela, 2008). This program was planned around 1790 (Furtado, 1994). It started in Portugal in 1802 with the renovation and operation of the blast and refining furnaces of the *Ferraria de Foz D'Alge* (Medeiros, 2009). In 1807, the Portuguese royal family and its court of nearly 15,000 people departed from Lisbon towards Rio de Janeiro, just a few days before Napoleon Bonaparte invaded Lisbon. From 1808 until 1821, they remained in Rio de Janeiro, which functioned as Portugal's Kingdom's capital. Between 1809 and 1822, the Portuguese "ironmaking & steelmaking" program continued in Brazil with the construction of The Morro do Pilar Iron Factory (Araújo, 2014) and The Patriótica Iron Factory, both in Minas Gerais, together with The Royal Iron Factory of *São João de Ipanema* in São Paulo (Araújo et al., 2010; Landgraf and Araújo, 2014).

"At this time, the carpenters and masons were almost ready, so on December 17th, 1812, I was able to make the first iron bars in Brazil. I received six men to teach. I started to melt and forge day and night until they learned. Nevertheless, they have not yet learned it properly, and I have already received orders from the king to leave this plant to go to another plant."

At that time, expressions associated with the verb "to melt" were used even when referring to iron oxide's solid-

state transformation into metallic iron. Nowadays, the verb "to melt" is used as a synonym for the solid to liquid phase transformation, while the verb "to cast" is used to describe the technique of pouring liquid metal into moulds to obtain a component. In Portuguese, however, the verb "fundir" has the same meaning of "to cast" and "to melt". The old usage of the verb "to melt" has caused some confusion among contemporary readers, who interpreted this description as if The *Patriótica Iron Factory* had produced pig iron. However, the *Factory* never produced molten iron, as the blast of unheated air over the red-hot coal reaches a maximum temperature of 1200 °C, which is well below the melting temperature of the pure iron, around 1538 °C. The production of liquid iron was only possible in the blast furnace, and the furnaces of *Patriótica* were not tall enough to produce it (Miller, 1976; Landgraf *et al.* 1994; Jockenhövel and Willms, 1997).

Eschwege (1979) knew from his past experiences in Germany and Portugal that a blast furnace's operation required continuous work (24 hours a day and seven days a week; it could not be interrupted). Additionally, the blast-furnace would produce 300 tons of iron per year, twenty times larger than the production he had devised for *Patriótica* according to the local demand (15 tons of iron per year). In the year 1800, the world consumption of iron (Hildebrand, 1957) was around 1 million tons per year, with England consuming 150,000 and France 35,000 tons of iron per year. The estimated Brazilian consumption was merely about 2,000 tons of iron per year. Varnhagen (Eschwege, 1979) wrote that São Paulo province imported 200 tons of iron per year. Simultaneously, Minas Gerais province, which had a larger population than São Paulo, imported only 100 tons of iron per year. Eschwege, 1979 argued there was neither the demand nor the logistics to distribute a large amount of iron in Minas Gerais.

According to Eschwege (1979), four "Swedish type" reduction furnaces were built in the *Patriótica Iron Factory*. These furnaces were approximately 1.5 m in height, while the furnaces built by the Swedish company in the Royal Iron Factory of *São João de Ipanema* were around 1.9 m in height and 44 cm in internal diameter, as described by Vergueiro (1822). The process for the production of "iron bars" was composed of two stages. The first stage, a reduction stage, took place inside the furnace.

The iron oxide was heated between 1100 and 1200 °C and reacted with the carbon monoxide produced by the coal's burning. The result was the production of metallic iron. Simultaneously, the ore's impurities, charcoal ashes and furnace lining reacted with the iron oxide, forming a viscous liquid slag, which, during its solidification, was trapped in the pure iron. The second stage took place outside the furnace, and the iron-slag solid was reheated so that the semi-liquid slag could be expelled from the iron during the hammering (Miller, 1976). The first stage took place inside one of the furnaces, see Figure 1-c. According to Eschwege (1979) description, the furnace was a large parallelepipedon built in stone, just over 1.5m tall, with a vertical cavity in the middle (see black circles in Figure 2). At its base, called the crucible, the furnace featured a square section (side of 60 cm), and its loading mouth was narrowing until it reached an area of 64 cm². In other words, the furnace would be a pyramid trunk with the largest base facing downwards. This furnace geometry is unusual compared to the most common designs of the time, including the Osmund furnace (Swedenborg, 1734; Dupré, 1885). The Osmund furnace is the best-known Swedish type furnace described by Swedenborg (1734) in a text reproduced by Percy (1865). This furnace type featured a square section, which extended upwards, while iron bloom removal was performed in its lower part.

The rich iron ore found in the area near *Patriótica*, which contains a maximum of 5% of impurities (mainly SiO₂), was added in alternating layers with charcoal inside the furnace's vertical cavity. Eschwege (1979) did not mention the use of fluxes, along with iron ore and coal. It was common to add to the load a certain amount of minerals called "fluxes" to lower the slag's melting point and facilitate its removal during the hammering operation. The proportion of iron ore, coal, and fluxes varied widely, depending on the type of iron ore and raw materials found in each region. The British, since 1700, for instance, have used coke from mineral coal. The iron ore, coal, and fluxes could be loaded in the furnace in many combinations, usually in iron ore and coal layers. So were the numerous ways to remove the spongy solid mass of pure iron from the furnace. It is impossible to understand the details of the direct reduction processes used in each iron producer based on the name of a furnace (Miller, 1976; Percy, 1865).

Eschwege (1979) credited himself

with implementing an essential innovation in the air admission system into the furnace. He wrote that among the various "enterprises" he visited in Minas Gerais, only one *Factory* did not use manual bellows: "Itabira do Mato Dentro was the only place where there was a kind of closed-chest furnace, whose air was supplied by a large leather bellows, driven by a water wheel." The innovation implemented by Eschwege (1979) was using the water trompe to blow pressurised air into the furnace to increase its productivity. The water, flowing down a pipe with holes, sucked in the air due to the Venturi effect. When the water containing the air bubbles fell into a sealed wooden box, the water and air were separated. The pressurised air exited through a hose leading to the "algaraviz" (the tube that injected forced air into the furnace). In this way, a continuous and pressurised flow of moisturised air was blown into the furnace. The air pipes' position and their injection angle were essential factors for the efficiency of the direct reduction process. Such a method of injecting forced air in the reduction furnaces has an Italian origin back in the 17th century, being adopted in the Catalan forges (Tomas, 1999) and later in the USA. Eschwege (1979) stated that he had no previous experience with this process of pressuring the air into the furnace:

"At that time, I still did not know the work of the trompes. The necessity forced me to adopt (the trompes) because of the foreseen difficulties I would have to struggle due to the lack of knowledge in the manufacture of bellows."

The introduction of this air insufflation technique had an essential impact on the metallurgy of Minas Gerais province. Almost seventy years later, in 1881, a student at the School of Mines of Ouro Preto, Joaquim Sena, described the iron factories he found on a trip from Ouro Preto to Diamantina. Sena described 21 factories in operation (Sena, 1881), with a daily production of between 60 and 200 kg of iron, which operated according to two processes, one of which is as follows:

"In these forges, iron is prepared in furnaces that they commonly call crucibles and which belong more or less to the type of furnace "a la manche". I don't know what the origin of such furnaces can be attributed to; it seems to me that after the great Factory founded by the intendant Câmara in Morro de Gaspar Soares was extinct, the curious who wished to continue the iron metallurgical industry, not having enough knowledge to assemble forges in

the "Catalan system", arrived finally to the iron preparation system in the crucibles."

There is a direct link between the process used by Eschwege (1979) at the Patriótica and the one used by the intendante Câmara after his blast furnace cracked and clogged. The former technician of Eschwege at the Patriótica, Johann Schönewolf, was invited to work at the iron factory located at Morro de Gaspar Soares and wrote in a letter (Eschwege, 1979), "One of the small furnaces is already assembled, and the respective hydraulic trompe, as I indicated." Returning to Sena (1881), he did not clarify if any of the furnaces he found in the 21 ironworks between Ouro Preto and Diamantina used the water trompe system to insufflate air into the furnaces. In one of the descriptions, he stated, "blowers supply the air". When describing another factory, which used a different process than the crucible, the Italian process, he affirmed, "The wind necessary to reduce the ore is supplied by a tuyere analogous to that of the Catalan system". The Catalan system has, characteristically, the production of forced air by water trompes. In another excerpt, he commented that in one of the factories, "nine work with blowers and the rest with bellows," which reinforces the interpretation of what he calls the "water trompe."

Three years later, Ferrand (1884a) described the two methods cited by Sena (1881): the crucible method (cadinho

method) and the Italian method. In his description of the crucible method, he made clear that

"a forge is usually made up of one to two furnaces containing 3 or 4 crucibles, —one to two reheating forges, similar to our blacksmith's tents. A hammer moved by a hydraulic wheel. Two trompes to send the forced air, one to the crucibles, the other one to the reheating forge".

The drawings made by Ferrand (1884a) to describe a typical ironwork using the crucible method were very similar to the floor plan shown in Figure 2 (Eschwege, 1979):

"The furnaces were loaded with layers of coal and ore, in loads of 4 kg. The furnace's operation, burning the coal, caused the load to go down inside the furnace. These loads were carried out whenever the level difference between the mouth and the last load reached 30 cm. Eschwege says that up to 18 charges were needed to obtain a lump of 22 kg of metallic iron finally. He even states that the coal consumption per kg of iron was around 14 to one (average in 5 years of operation). This data shows one of the biggest challenges in iron production at that time."

The description of the "cadinho" furnaces, made by Ferrand (1884b), was published in the French magazine *Le Génie Civil* in 1883 and republished by the *Scientific American* in 1884, reflecting the

originality of this solution. As Eschwege (1979) described, the interior void profile of the furnace differs slightly from the drawing of Ferrand (1884a, 1884b). Figure 3 reproduces the proposed design by Horstmann and Toussaint (1989) in an article about the Patriótica Iron Factory. The hole in the "algaraviz" is placed at a much higher height than Ferrand's drawing, but it corresponds to the height described by Eschwege (1979).

Most of the literature assumes that the Patriótica Iron Factory closed down when Eschwege returned to Portugal in 1821, but there is proof of its prolonged survival up to 1831 (Libby, 1988). The seven pages of the chapter "Geschichte der Eisenhütte do Pratta bei Congonhas do Campo in der Provinz Minas Geraes" are the leading reference on the manufacturing process adopted in the Patriótica Iron Factory (Eschwege, 1979). In the German edition, the Factory's name is changed from Patriótica, the name registered in Brazil, to Pratta. All later commentators of the Patriótica Iron Factory, as Calógeras (1904) and Gomes (1983), practically repeated what Eschwege (1979) had described, except a few additions by Baeta (1973). This means that there is not much additional information about iron processing in the Patriótica Iron Factory. In this sense, one of the aims of the present investigation is to gather further information about the manufacturing processes.

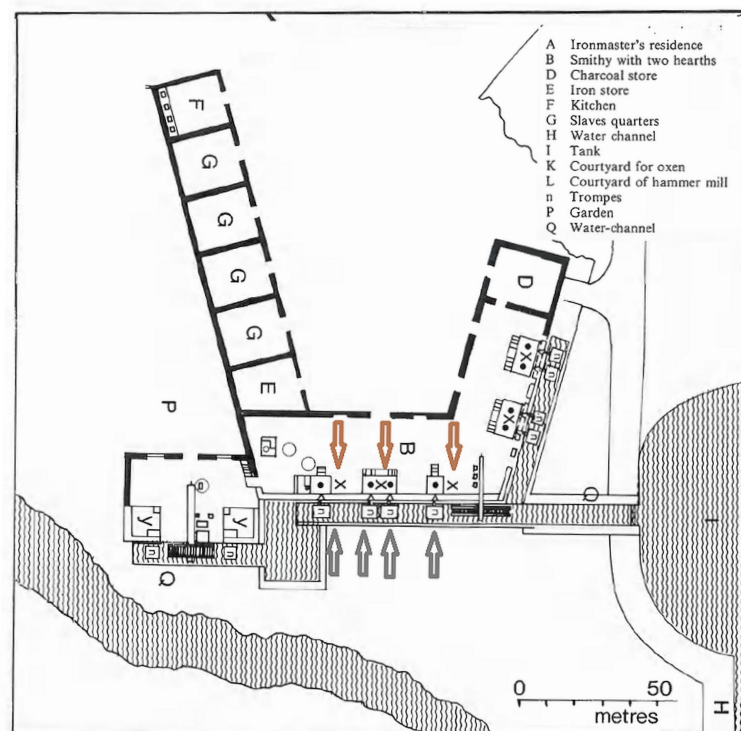


Figure 2 - The layout of The Patriótica Iron Factory and the position of the reduction furnaces (see X and red arrows in section B). The black circles represent the "mouth" of the furnaces, and the grey arrows show the position of the water-driven air trompes of the four reduction furnaces (Pinho and Neiva, 2012; Eschwege, 1979).

Spiked to the stones of the reduction furnaces found in the Patriótica Iron Factory remnants, one finds at least three iron eyebolts. There are four iron pieces on the side of furnace number one, one of which can be identified as the hammer's head. Ferrand (1884a, 1884b) published a drawing of the hammer typical of the crucible forges of Minas Gerais. According to Ferrand (1884a, 1884b), the hammers were

always driven by water wheels. In that drawing, the axis of the water wheel is parallel to the hammer rod. There, he shows the hammer's iron head and anvil, similar, but not equal, to that found in the Patriotic Factory. Sena (1881) noted the weight of hammers for each of the 21 forges visited ranged between 80 and 180 kg, and the number of "strokes per minute" varied between 80 and 200. In the elevation

drawing, Ferrand's scheme does not show the lifting mechanism of the hammer rod. In the pictures by other authors this mechanism consisted of four iron cams on the wheel axle, which, when rotating, raised and dropped similar cams on the hammer rod. Neither Eschwege (1979), nor Sena (1881), nor Ferrand (1884a; 1884b) informed how many centimetres the hammer's head rose above the anvil.

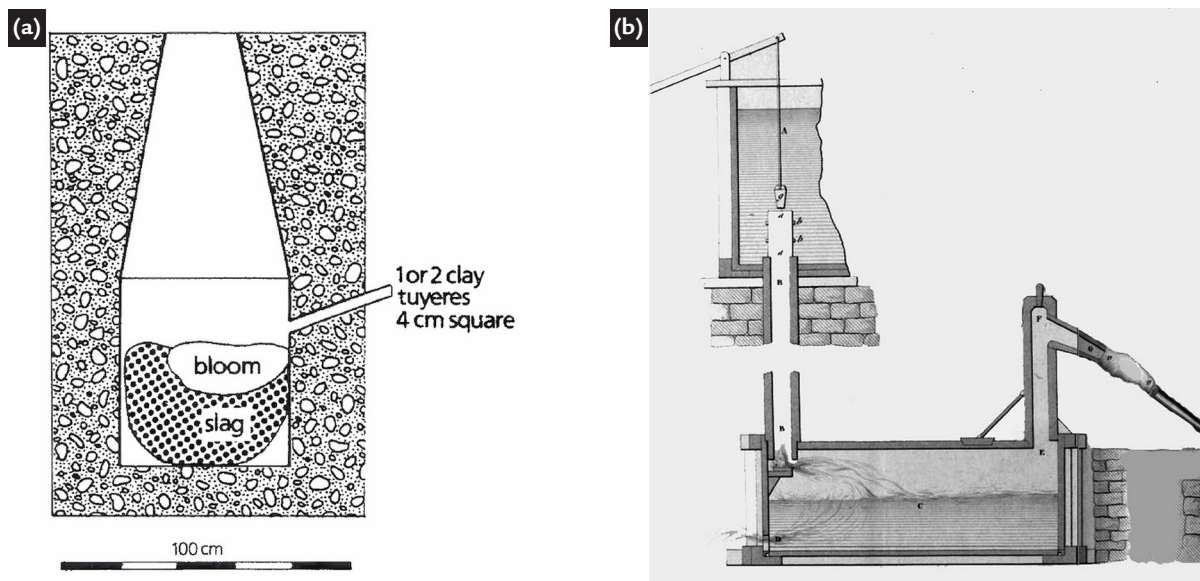


Figure 3 - (a) Profile of the reduction furnace of The Patriótica Iron Factory interpreted by Horstmann and Toussaint (1989); (b) Water-driven air trompes (François, 1843).

Drawings made by Ferrand (Ferrand, 1884a; Ferrand, 1884b) depicts a hammer used in iron factories at the end of the XIX century (see Figures 4-a and 4-b). This hammer should not be much different than the one used by Eschwege (1979) in the Patriótica Factory. Today, by the side of a furnace remnant, lies an iron piece that must have been the iron head of that hammer (see dimensions and geometry in Figure 4-a). Next to the hammer's head (see upper right of the figure), another piece of iron is probably the anvil. Eschwege

(1979) did not explain the origin of the iron hammer of the Patriótica Iron Factory in his book, but in 1904 Calógeras (1904), a former student of the School of Mines of Ouro Preto, stated:

“These hammers were the ones that the ministry had imported from England in 1810, on the advice of Eschwege and according to measures given by him, to overcome the difficulty of forging new devices like these, anvils, crops, etc. with simple hand hammers”.

Another piece of information

concerning the hammer comes from Baeta (1973), who reports a letter from the governor of Minas Gerais detailing a visit made in 1813, in which the governor mentions that the hammer from England had broken, but that provision was made for “the making of a new hammer, whose work was considered invincible”. If that hammer was imported from England in 1810, as suggested by Calógeras (1904), it could have been produced by either a direct reduction process or pig iron refining.

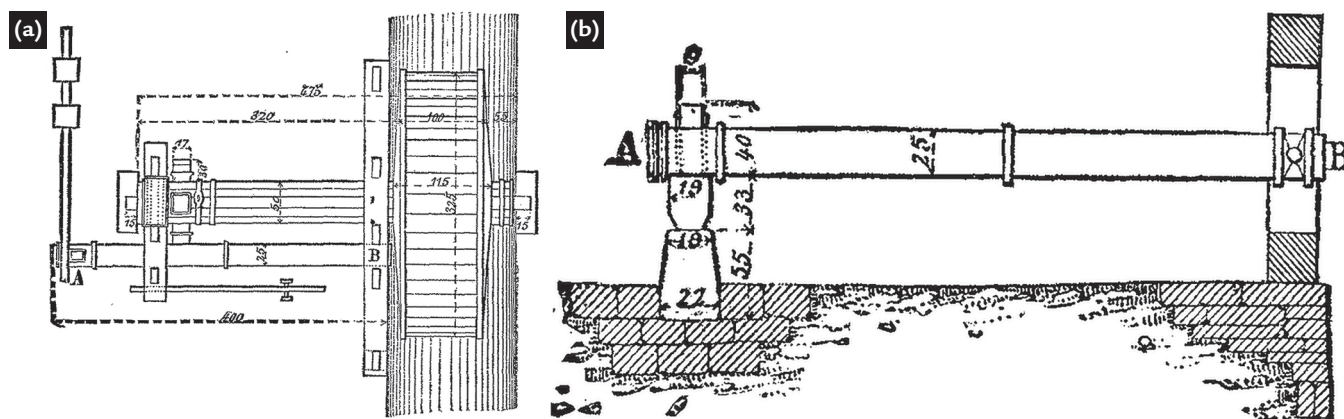


Figure 4 - Hammer of a crucible forge, according to a drawing published by Ferrand (1884a; 1884b). (a) Position of the hammer's iron head (A) on the floor plan, showing the water wheel (right); (b) A-B cross-section, indicating the position of the iron head in the hammer (left).

1.3 Slag inclusions

The direct iron ore reduction process occurs with the iron ore in solid-state, without forming a liquid iron phase, using charcoal and carbon monoxide as reductants agents. The reduction process produces sponge iron, containing large amounts of entrapped slag inclusions (the iron ore impurities are mixed with iron oxide). This sponge is hammered to adjust the shape and expel the excess semi-liquid slag out of the metallic iron (Miller, 1976; Eschwege, 1979; Ågren, 1998; Agricola, 2011). The pig iron refining, so-called the indirect process, could be done in different ways, as described by Percy (1864), but always passing through a solid-state forging step to expel the oxidising slag needed to lower the carbon content. Dillmann and L'Héritier (2007) noticed that samples produced by the indirect process have higher phosphorous content in the slag due to the easy reduction of that element and dilution in the pig iron. The hammering process does not remove all the slag entrapped in the iron bar, producing a ferrous artefact, whose microstructure of metallic iron crystals contains a hetero-

geneous distribution of micrometric slag inclusions in volumetric fractions from 1 to 10%.

The slag inclusion's chemical composition can be used to examine the provenance of ferrous artefacts (Buchwald and Wivel, 1998; Dillmann and L'Héritier, 2007; Blakelock *et al.*, 2009; Charlton *et al.*, 2012; Maia *et al.*, 2015; Mamani-Calcina *et al.*, 2017). Ferrous products manufactured before the twentieth century contain large amounts of slag inclusions in their microstructure. These inclusions feature various phases, each composed of a mixture of oxides. The chemical composition of these slag inclusions is defined by the composition of the different materials and raw materials used during the manufacturing process, such as iron ore, charcoal ash, furnace lining, fuel, hearth lining, fluxes, etc. The investigation of the slag inclusion chemical composition in ancient ferrous artefacts has been used to determine technological and historical characteristics of the metallurgical processing, including their possible provenance. Maia *et al.* (2015)

analysed the slag inclusions of ferrous objects collected from the Royal Iron Factory of São João de Ipanema and the Afonso Sardinha archaeological site. They suggested that the presence of higher contents of TiO_2 in the inclusions was a typical characteristic of the artefacts, which were collected in Sardinha's archaeological site. Mamani-Calcina *et al.* (2017) investigated the slag inclusions of ferrous artefacts of the Royal Iron Factory of São João de Ipanema, the D. Pedro II Bridge (XIX century, Bahia, produced in Scotland), and the archaeological sites of São Miguel de Missões (XVII century, Rio Grande do Sul, Brazil) and Afonso Sardinha (XVI century, São Paulo, Brazil). The slag inclusion microanalyses results were investigated by hierarchical cluster analysis. The dendrogram with the wüstite phase microanalyses results (using as critical variables the MnO , MgO , Al_2O_3 , V_2O_5 , and TiO_2 contents) allowed the identification of four clusters, which successfully represented the samples of the investigated sites (Ipanema, Sardinha, Missões and Bahia).

1.4 Scope of the investigation

The National Historic and Artistic Heritage Institute (IPHAN) and Vale S.A. authorised the removal of 1 cm^3 samples of the iron eye and the hammer for the microstructural investigation, which followed the procedures applied to other ferrous objects (Buchwald and Wivel,

1998; Dillmann and L'Héritier, 2007; Maia *et al.*, 2015, Mamani-Calcina *et al.*, 2017). The analysis of these samples' microstructure offers an opportunity to discuss the ironmaking techniques used 200 years ago. The examination of the historical and technical documents and

the microstructural investigation of the ferrous samples found in the Patriótica Iron Factory help us understand how the ferrous artefacts were fabricated and whether any of these two artefacts were manufactured in the Patriótica Iron Factory.

2. Materials and methodology

A ferrous 1 cm^3 sample of the iron eyebolt was collected close to the bottom of the charging face of furnace 3 (sample LCMHC 188, see Figure 1-a). Iron ore samples were provided by Vale SA, taken from their collection at the "Mina da Fábrica", the mine where the Patriótica Iron Factory is located (identification LCMHC 189, 190 and 191). In the Laboratory for Microstructural Characterisation "Hubertus Colpaert" (EPUSP), the ferrous sample was prepared for metallographic examination using a classic procedure (Maia *et al.*, 2015; Mamani-Calcina *et al.*, 2017). The

unetched and etched polished surfaces were observed using optical and scanning electron microscopes (Quanta 450 FEG), the latter equipped with energy dispersive spectrometry (EDS) microanalysis. The slag inclusion volume fraction was determined by the grid method. The ferrous samples were etched by a 2% Nital solution to reveal the microstructure of the iron. The EDS microanalyses of the multiphase slag inclusions were carried out on the main microstructural constituents of the inclusion and larger area representing the "entire" multiphase slag inclusion. Data

investigation of the EDS microanalysis (standardless mode, a voltage of 20 kV, spot and area modes, 4.5 spot size, 30 seconds collection time, and ZAF correction) used the TEAM EDS Analysis System software. A restriction for the quantitative chemical analyses was imposed by assuming that all the chemical elements present in the slag inclusions were in the form of oxides. Finally, the iron ore samples were analysed by an X-ray fluorescence spectrometer (PANalytical, Zetium) at the Laboratory for the Technological Characterisation (EPUSP), using the standardless method.

3. Results

3.1 Eyebolt

Figure 5-a indicates the eyebolt sampling near the bar's bend, featuring a triangular cross-section, and Figure 5-b

shows the polished surface parallel to the horizontal surface of the eyebolt. The base of the triangular cross-section is the

bend and oxidised surface of the eyebolt, while its opposed vertice is near the centre of the bar. The eyebolt was made from a

square-section bar, which was bent by forging, and the slag inclusions (dark strings) follow the plastic flow of the iron

during the plastic deformation of the bar. The volume fraction of slag inclusions is around 4.0%, but their size and volume

distribution change from the surface towards the bar's centre, where the slag inclusions are not so elongated.

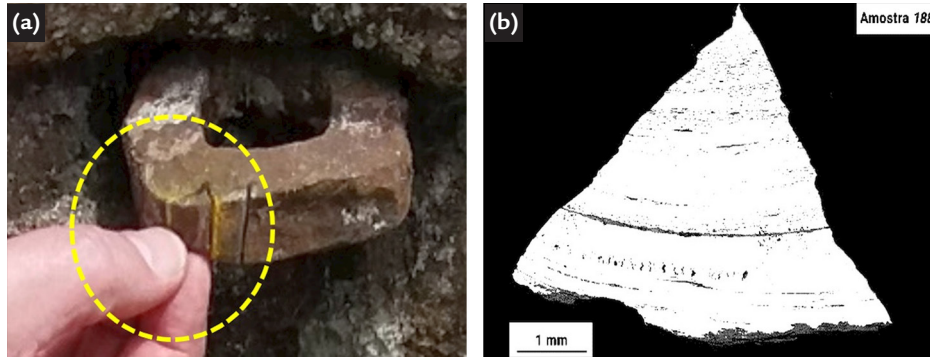


Figure 5 - Eyebolt (LCMHC 188). (a) Sampling; (b) Polished surface of the eyebolt, showing aligned slag inclusions (see dark regions). Optical microscopy, unetched.

Figure 6-a shows aligned and elongated slag inclusions near the surface of the eyebolt. There are at least two phases within each inclusion. There are globules (medium-grey regions) surrounded by a dark-grey matrix, and their proportion and morphology can vary in each slag inclusion. The microstructure of the iron matrix of the eyebolt is shown in Figure 6-b. There is a mixture of parallel plates of ferrite (Yin *et al.*, 2017) and perlite (the dark region between the plates) close to the bar's surface (bottom of the figure),

while the interior of the bar shows equiaxial grains of ferrite without pearlite. The pearlite presence indicates that the carbon content near the surface is higher than in the iron bar's centre. Figures 7-a to 7-d show three different types of slag inclusions found in the eyebolt: quasi single-phase microstructure (Figure 7-a); duplex microstructure (Figure 7-b); and single-phase microstructure (Figure 7-d). The results of the EDS microanalysis are shown in Table 1. The quasi single-phase inclusions, Figure 7-a, contain the dominating presence

of the wüstite (FeO), phase (light-grey region, see 1), almost 50 µm in length, surrounded by a small amount of a SiO₂-rich matrix (dark-grey area, see 2 and 3). The matrix of the quasi single-phase inclusions shows a much lower volume fraction than the duplex inclusions (5% vs 50%); see Figures 7-a and 7-b. This matrix is richer in SiO₂, Al₂O₃, CaO, MgO, P₂O₅, MnO and K₂O than the matrix of the duplex slag inclusions, suggesting it is composed of a vitreous phase (Tossavainen *et al.*, 2007; Jung and Sohn, 2014).

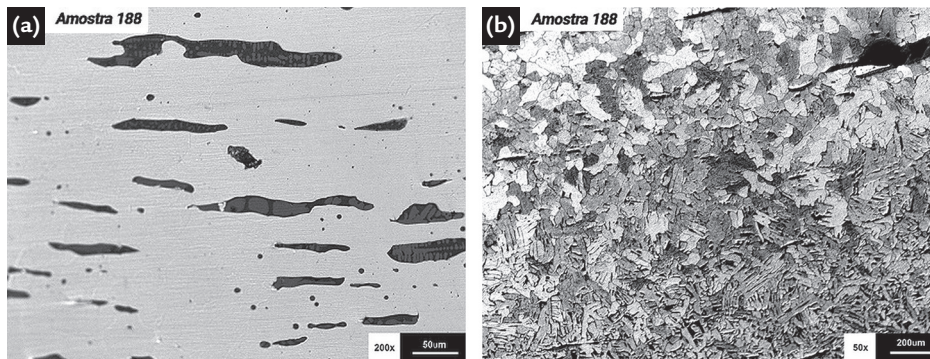


Figure 6 - Eyebolt (LCMHC 188). (a) Aligned and elongated slag inclusions. The inclusions show at least two phases (dark grey, globules, and medium-dark grey, matrix, regions). Optical microscopy, unetched; (b) Heterogeneous microstructure, showing close to the surface of the bar (see bottom of the figure) the presence of ferritic plates and perlite (dark region between the plates). The interior of the bar shows equiaxial grains of ferrite. The presence of pearlite indicates that the carbon content near the surface is higher than the centre of the iron bar. Etching, Nital 2%.

The duplex slag inclusions, Figure 7-b, feature an equal proportion of wüstite and matrix. However, at around 8000 times magnification, the microstructural observation of the matrix of the “duplex” inclusions reveals a dual-phase microstructure (see Figure 7-c). This microstructure contains a vast proportion of fayalite (Fe₂SiO₄), probably precipitated in a liquid that transformed into a vitreous phase ma-

trix. When the liquid slag pools trapped in the solid iron start to solidify, the first solid to form is a wüstite crystal (FeO), which grows freely inside the liquid slag, forming the wüstite dendrites (Figure 7-b). The morphology of the wüstite dendrites' arms, aligned in parallel (Figures 7-b and 7-c), suggests a single wüstite crystal. This dendritic morphology was not altered by the iron bar forging, implying that the forging

occurred at a temperature above the melting temperature of the slag (the melting temperature of the wüstite is 1371 °C, but the wüstite-fayalite eutectic is around 1183 °C, see Figure 8). Nevertheless, the hypothesis that the forging occurred after the slag's solidification cannot be ruled out, but the wüstite morphology does not indicate its plastic deformation. Moreover, the ionic crystals, such as the oxides,

present selective solubility, and the duplex slag inclusions (see Figure 7-b)

are an excellent example of this behaviour, since wüstite (FeO) does not

present a solid-solution of SiO_4^{-4} ions, see Table 1.

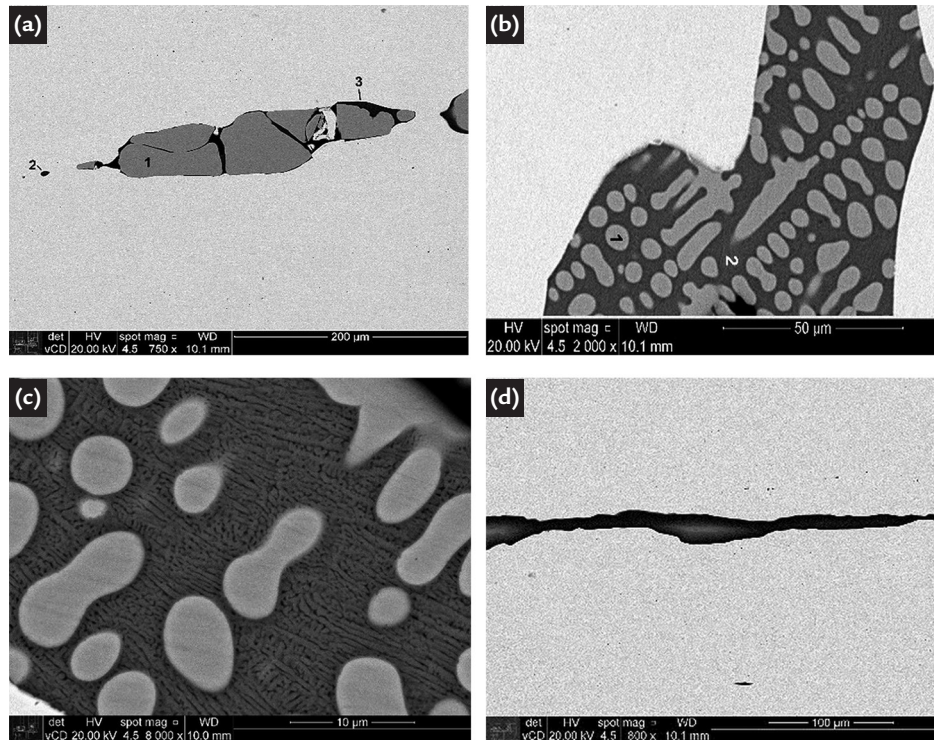


Figure 7 - Eyebolt (LCMHC 188), types of slag inclusions.

(a) Quasi single-phase microstructure inclusion, containing a large volumetric fraction of wüstite

(FeO, region 1) in a SiO_2 - Al_2O_3 -CaO-MgO- K_2O -rich vitreous phase matrix; (b) Duplex microstructure inclusion.

Region 1 shows the wüstite phase (FeO), and region 2 the SiO_2 - Al_2O_3 -CaO-MgO- K_2O -rich matrix.; (c) Detail of the slag inclusion shown in (b), the matrix features a dual-phase composed of fayalite ($2\text{FeO}\cdot\text{SiO}_2$) precipitates (main microconstituent) in a vitreous phase matrix; (d) Elongated single-phase microstructure inclusion, featuring a SiO_2 - Al_2O_3 -CaO-MgO- K_2O -rich vitreous phase. Scanning electron microscopy, back-scattered electron image (BEI), and EDS microanalysis (see Table 1). Unetched samples.

Table 1 - Results of EDS microanalysis of the phases present in the slag inclusions of the eyebolt sample.

The chemical compositions of the iron ore, the Patriótica's smelting slag and the charcoal ashes are also listed (weight %).

Type of slag inclusions and microconstituents	FeO	SiO ₂	Al ₂ O ₃	MgO	CaO	K ₂ O	P ₂ O ₅	TiO ₂	MnO
Quasi single-phase (Figure 7-a), position 1, globules, wüstite (FeO)	96.0	-	0.7	2.5	-	-	-	-	0.8
Quasi single-phase (Figure 7-a), position 2, vitreous matrix	38.3	32.0	10.0	3.5	8.2	3.0	1.8	-	1.4
Quasi single-phase (Figure 7-a), position 3, vitreous matrix	40.5	29.9	10.5	2.0	9.4	3.2	1.6	-	1.3
Duplex (Figure 7-b), globules, wüstite (FeO)	99.2	0.2	0.6	-	-	-	-	-	-
Duplex (Figure 7-b), matrix (fayalite, $2\text{FeO}\cdot\text{SiO}_2$, is the majoritarian phase)	65.3	27.5	4.5	0.6	1.3	0.8	-	-	-
Duplex (Figure 7-b), matrix (fayalite, $2\text{FeO}\cdot\text{SiO}_2$, is the majoritarian phase)	64.0	25.0	6.0	1.0	1.5	1.3	-	0.7	0.7
Single-phase (Figure 7-d), vitreous phase	7.8	50.6	18.3	5.6	9.3	4.3	-	1.2	2.8
Single-phase (Figure 7-d), vitreous phase	7.0	51.4	18.5	6.1	8.9	4.9	-	1.3	2.6
Iron ore, Patriótica Iron Factory mine, hematite ($*\text{Fe}_2\text{O}_3$)	98.3*	0.6	0.4	0.1	0.05	-	0.03	-	0.04
Slag from the Patriótica Iron Factory (Horstmann and Toussaint, 1989)	71.4	20.9	4.1	-	1.1	1.2	0.23	0.28	-
Charcoal ash (Dueñas-Gonzales, 2014)	2.0	11.1	12.2	4.5	42.8	22.5	0.04	0.4	2.8
Charcoal ash (Gomes, 2016)	4.4	9.6	6.6	10.8	40.8	7.4	-	0.8	0.7

Note: Na₂O, sulfur and V₂O₅, which are frequently found in the slag inclusions, were not found in the EDS microanalysis.

According to the FeO-SiO₂ phase diagram, see Figure 8 (Slag, 1995), during the slag's solidification, the growth of the wüstite dendrites expels the SiO₄⁻⁴ ions into the remaining liquid slag until the formation of the

wüstite-fayalite eutectic takes place at 1177 °C. The single-phase slag inclusions, Figure 7-d, feature a more elongated morphology. Their chemical composition (see Table 1), also richer in SiO₂, Al₂O₃, CaO, MgO, MnO, TiO₂

and K₂O than the SiO₂-rich matrix of the duplex slag inclusions, suggests that the single-phase is a vitreous phase, which did not crystallise during the solidification (Tossavainen *et al.*, 2007; Jung and Sohn, 2014).

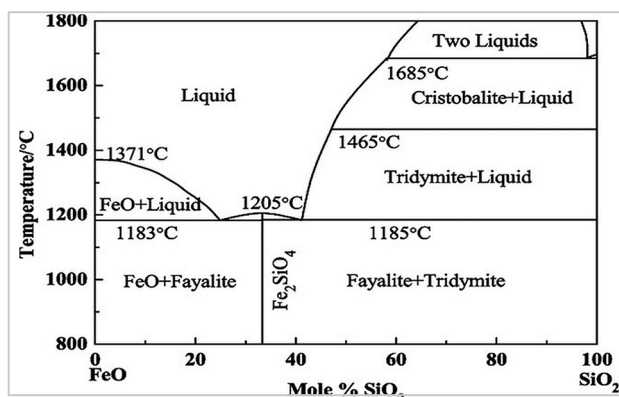


Figure 8 - FeO-SiO₂ phase diagram (Slag, 1995).

EDS results (Table 1) indicated that the chemical composition of the same microconstituent for the same type of slag inclusion is roughly the same. In contrast, different types of slag inclusions show different chemical compositions for similar microconstituents. For instance, the matrix of the quasi single-phase inclusions features lower FeO content than the matrix of the duplex inclusions

(40% vs 65 %). In contrast, the Al₂O₃, MgO, CaO and K₂O contents of the matrix of quasi single-phase inclusions are comparatively higher than the matrix of duplex inclusions (10% vs 5%, 3% vs 0.8%, 9% vs 1.4% and 3% vs 1%, respectively). These results suggest that the quasi single-phase and duplex slag inclusions have different origins in the iron bar's manufacture (reducing and

forging steps). The present investigation was not able to identify the provenance of each type of inclusion. The various oxides found in the slag inclusions could be originated from the clay used for the furnace lining (Al₂O₃, SiO₂, and TiO₂); the fuel ashes of the charcoal (MgO, K₂O, and CaO); the smithing flux (SiO₂); and the iron ore (iron oxide and other impurities) (Charlton *et al.*, 2012).

3.2 Hammer

Figure 9-a indicates the hammer's sampling position, and Figure 9-b shows the polished surface of a section of the hammer sample. The distribution of the slag inclusions within the

hammer is more heterogeneous than the eyebolt sample, and its volumetric fraction is around 2.8%. The volumetric fraction of slag inclusions found in the hammer samples is within the range

observed in iron objects produced in the world until 1890, before spreading the new refining techniques that revolutionised the world steel industry (Tylecote, 1984).

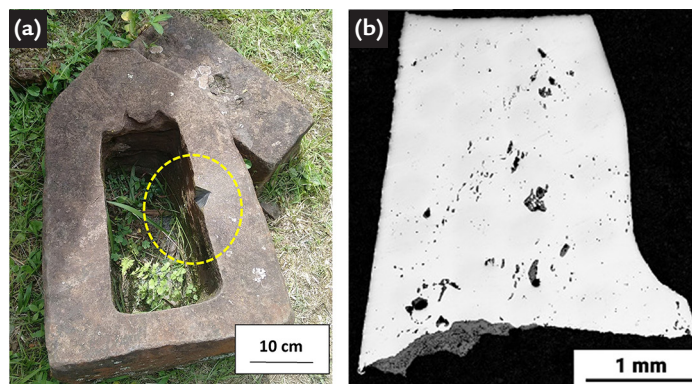


Figure 9 - Hammer (LCMHC 193). (a) Sampling position, dotted area (thickness of the hammer is around 46 cm); (b) Polished surface of the, showing the slag inclusions (dark regions) with various sizes and heterogeneous distribution. Optical microscopy without chemical etching.

Figures 10-a and 10-b reveal that the slag inclusions of the hammer have different sizes and morphologies. Still, they are all similar in appearance, always containing large amounts of the globular phase (medium-grey regions) previously indicated

as wüstite dendrites in literature (Gordon, 1997; Buchwald and Wivel, 1998; Dillmann and L'Héritier, 2007; Blakelock *et al.*, 2009; Charlton *et al.*, 2012; Maia *et al.*, 2015; Mamani-Calcina *et al.*, 2017). The wüstite dendrites are surrounded by a small amount

of other darker phases. Figure 10-b shows, for instance, that solid-state precipitation of another phase took place inside the primary wüstite dendrites (see medium grey platelets identified as 2). The EDS microanalysis, see Table 2, indicated the presence of wüstite

(FeO) (see region 1 in Figure 10-b) and magnetite (Fe_3O_4) precipitates (see region 2 in Figure 10-b). Additionally, the precipitation of an iron halo, see region 5 in Figure 10-b, was observed between the primary wüstite dendrite and the interdendritic region. The Fe-O phase diagram (Nadoll and Mauk, 2011), see Figure 11, shows that the wüstite phase is not stable below 570 °C, decomposing into iron (ferrite) and magnetite (Fe_3O_4) below the eutectoid temperature, explaining the presence of Fe_3O_4 platelets and the ferrite halo in the slag inclusion microstructure. Previous accounts of this eutectoid decomposition in the wüstite dendrites of iron artefacts have not been found in the archaeometallurgical literature.

Figure 10-b also indicates that the interdendritic region also presents two phases

(see regions 3 and 4). Table 3 shows the EDS microanalysis results of these two phases, indicating the presence of fayalite (dark-grey region, 3) and a glassy phase (black region, 4). The chemical composition of the fayalite ($2\text{FeO} \cdot \text{SiO}_2$) phase shows that this phase did not dissolve as much Al_2O_3 (0.5% vs 4.5%) nor K_2O (0% vs 0.8%) as the eyebolt duplex inclusion, see Table 4. The MgO (1.4% vs 0.6%) and MnO contents (0.7 vs 0%) in the fayalite are higher in the hammer than in the eyebolt. The chemical composition of the “black” phase, region 4 in Figure 10-b, corresponds to the leucite ($\text{K, Al}(\text{Si}_2\text{O}_6)$) phase. This region has been interpreted in literature as a vitreous phase (Horstmann and Toussaint, 1989). The vitreous phase in the hammer features much higher contents of SiO_2 (38.3% vs. 29.9%), Al_2O_3 (27.5%

vs 10.5%) and K_2O (24.2% vs 3.2%) and lower contents of MgO (0% vs 2.0%), CaO (2.5% vs 9.4%), MnO (0% vs 1.3%) and P_2O_5 (0% vs 1.6%) than in the vitreous matrix of the quasi single-phase inclusion of the eyebolt. Additionally, the vitreous phase in the hammer features much higher contents of Al_2O_3 ((27.5% vs 18.3%) and K_2O (24.2% vs 4.3%)) and lower contents of SiO_2 (38.3% vs 50.6%), MgO (0% vs 5.6%), CaO (2.5% vs 9.3%) and MnO (0% vs 2.8%) than in the single-phase inclusion of the eyebolt. The absence of phosphorous in the vitreous phase of the hammer is evidence that this component was not produced by the refining of pig iron. These microanalysis results suggest that the eyebolt and the hammer were fabricated in different production sites.

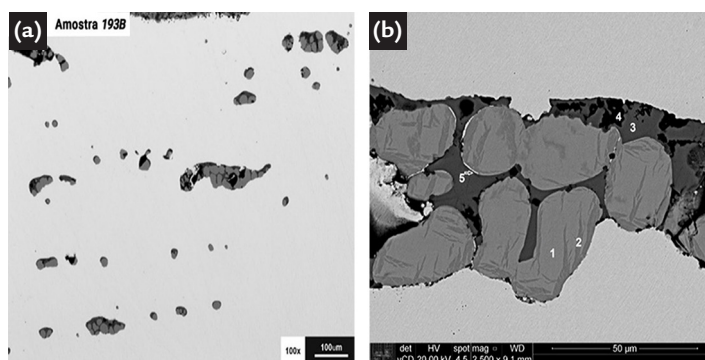


Figure 10 - (a) Hammer (LCMHC 193), slag inclusions. The inclusions show at least two phases (dark grey, globules, and medium-dark grey, matrix, regions). The slag inclusions are not as elongated as the eyebolt's inclusion. The proportion of the inclusions' globular phase is higher than the inclusions' matrix. Optical microscopy without chemical etching; (b) Detail of a slag inclusion showing five phases: (1) wüstite (FeO); (2) magnetite (Fe_3O_4), (3) fayalite (Fe_2SiO_4), (4) vitreous $\text{SiO}_2\text{-Al}_2\text{O}_3\text{-K}_2\text{O}$ phase, and (5) ferrite halo. Scanning electron microscopy, back-scattered electron image. Unetched sample.

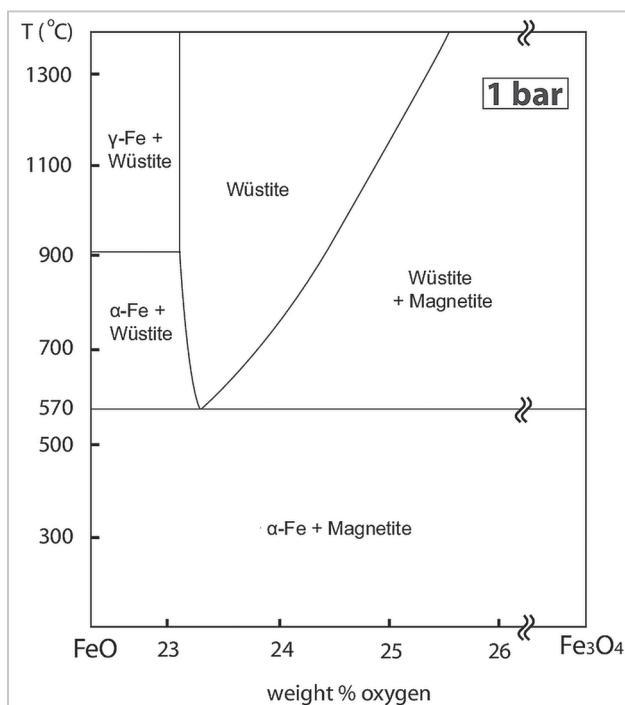


Figure 11 - Fe-O phase diagram, showing the eutectoid decomposition of wüstite (FeO) below 570 °C into magnetite (Fe_3O_4) and ferrite, adapted from (Nadoll and Mauk, 2011).

Table 2 - EDS microanalysis results of (at %) of the wüstite and magnetite phases (see regions 1 and 2 in **Figure 10-b**) in three slag inclusions of the hammer (LCMHC 193).

Slag inclusions	Fe	O	Si	Al	Mg	Ti
Inclusion A, phase 1, wüstite (FeO)	51.0	48.4	0.2	0.3	-	-
Inclusion B, phase 1, wüstite (FeO)	48.5	50.1	-	0.4	0.4	-
Inclusion C, phase 1, wüstite (FeO)	49.5	50.5	-	-	-	-
Inclusion A, phase 2, magnetite (Fe ₃ O ₄)	45.1	53.4	-	0.7	-	0.3
Inclusion B, phase 2, magnetite (Fe ₃ O ₄)	45.5	53.9	-	0.5	-	-
Inclusion C, phase 2, magnetite (Fe ₃ O ₄)	45.0	55.0	-	-	-	-

Table 3 - EDS microanalysis results (at %) of fayalite and vitreous phases (see regions 3 and 4 in **Figure 10-b**) analysed in five slag inclusions of the hammer (LCMHC 193).

Slag inclusions	FeO	SiO ₂	Al ₂ O ₃	K ₂ O	MgO	CaO	MnO
Inclusion A, phase 3, fayalite (Fe ₂ SiO ₄)	67.2	28.9	-	-	3.1	0.9	-
Inclusion B, phase 3, fayalite (Fe ₂ SiO ₄)	67.8	28.7	-	-	2.2	0.9	0.4
Inclusion B, phase 3, fayalite (Fe ₂ SiO ₄)	66.7	28.9	0.8	-	1.9	1.2	0.5
Inclusion E, phase 3, fayalite (Fe ₂ SiO ₄)	63.8	28.4	-	-	1.7	0.8	0.5
Inclusion F, phase 3, fayalite (Fe ₂ SiO ₄)	70.2	26.2	0.5	-	1.4	1.0	0.7
Inclusion G, phase 3, fayalite (Fe ₂ SiO ₄)	63.8	27.8	1.0	1.0	1.4	5.0	0.4
Inclusion A, phase 4, SiO ₂ -Al ₂ O ₃ -K ₂ O phase	7.3	38.3	27.5	24.2	-	2.5	-
Inclusion E, phase 4, SiO ₂ -Al ₂ O ₃ -K ₂ O phase	17.7	34.2	24.5	21.3	-	2.2	-
Inclusion F, phase 4, SiO ₂ -Al ₂ O ₃ -K ₂ O phase	9.5	42.0	26.5	21.2	-	0.9	-
Inclusion G, phase 4, SiO ₂ -Al ₂ O ₃ -K ₂ O phase	4.3	38.3	30.3	27.2	-	-	-

Note: Na₂O, SO₃ and V₂O₅ were not present, which are frequently found in slag inclusions.

Table 4 - EDS microanalysis, slag inclusions of eyebolt (LCMHC 188) versus hammer (LCMHC 193).

Slag inclusion	FeO	SiO ₂	Al ₂ O ₃	K ₂ O	MgO	CaO	MnO	P ₂ O ₅
Hammer, inclusion F, phase 3, fayalite (Fe ₂ SiO ₄), Figure 10-b	70.2	26.2	0.5	-	1.4	1.0	0.7	-
Eyebolt, SiO ₂ -rich matrix, fayalite*, duplex slag inclusion, Figure 7-b	65.3	27.5	4.5	0.8	0.6	1.3	-	-
Hammer, inclusion A, phase 4, SiO ₂ -Al ₂ O ₃ -CaO-K ₂ O vitreous phase, Figure 10-b	7.3	38.3	27.5	24.2	-	2.5	-	-
Eyebolt, SiO ₂ -Al ₂ O ₃ -CaO-K ₂ O rich vitreous phase, quasi single-phase inclusion, matrix, Figure 7-a	40.5	29.9	10.5	3.2	2.0	9.4	1.3	1.6
Eyebolt, single-phase inclusion, SiO ₂ -Al ₂ O ₃ -CaO-K ₂ O vitreous phase, Figure 7-d	7.8	50.6	18.3	4.3	5.6	9.3	2.8	-

Note: As the volumetric proportion of fayalite in the dual-phase (fayalite + glass) microstructure is very high, it has been assumed that the fayalite's chemical composition is very close to the chemical composition of the SiO₂-rich matrix.

4. Discussion

4.1 Eyebolt

One of the objectives of this research is to examine the hypothesis that the iron bar used for the eyebolt production was produced at the Patriótica Iron Factory. The EDS results of the three types of slag inclusions found in the eyebolt were compared to the raw materials used in the iron manufacturing process (Eschwege, 1979)

and the previous analysis of ferrous objects (bloom and slag/iron sponge) produced at the Patriótica Iron Factory (Horstmann and Toussaint, 1989), see Table 1. This article follows an approach initiated by Mamani-Calcina *et al.* (2017), analysing the chemical composition of each phase of the slag inclusions' microstructure. This article

also studies the different types of slag inclusion microstructures (single-phase, quasi single-phase and duplex) found in the eyebolt.

It is necessary to imagine how the eyebolt's iron bar was manufactured in order to understand the presence of at least three different types of slag inclusions (see Figures 7-a to 7-d), The

reduction furnace is not the Catalan type, where the iron bloom is taken by the open top. Instead, it was charged from the top and discharged in a bottom opening. It was loaded with alternate layers of iron ore and charcoal. The continuous burning of coal at the bottom of the lower part of the furnace makes room for the iron ore to descend along the furnace's height. The heated iron oxide particles are slowly reduced into iron from the surface to the centre by the carbon monoxide. One of the main differences among the three types of slag inclusions is the FeO content (see Table 1), which is maximum in the quasi single-phase slag inclusions and minimum in the vitreous single-phase slag inclusions. It is still unclear whether the FeO's presence in the slag results from the incomplete reduction of the ore (Fe_2O_3) or due to the reoxidation of the iron. The reoxidation could occur during the iron's passage at the air blast or by the iron's exposure to the air between the bloom removal and the forging process onset.

Evidence of the different reducing conditions in the bloom can be found in the eyebolt's metallographically etched images. Figures 6-a and 6-b show areas near the eyebolt surface, indicating the presence of two very different parts: the large duplex slag inclusions are associated with the equiaxed ferrite, indicating that the carbon content around these inclusions is less than 0.02%. The single-phase vitreous inclusions are usually surrounded by a ferritic-pearlitic microstructure (higher carbon content), similarly to what has been found in literature (Buchwald and Wivel, 1998).

EDS microanalysis of the different phases of the eyebolt's slag inclusions (Table 1) revealed that the FeO-rich wüstite dendrites dissolved small amounts of Si, Al, Mn and Mg. The matrixes of the quasi single-phase and duplex slag inclusions dissolved many oxides, such as FeO, SiO_2 , Al_2O_3 , MgO, K_2O and CaO. Small amounts of P_2O_5 and MnO (from 0 to 1.8%) and TiO_2 (from 0 to 1.3%) were also observed in these matrixes. When the slag inclusions feature a more significant presence of other elements rather than FeO, such as Al_2O_3 , MgO, CaO, and K_2O , they segregate into the remaining liquid slag, promoting the formation of a vitreous phase during solidification. Tossavainen *et al.* (2007) studied the effect of different cooling conditions on crystallisa-

tion in an oxide melt. They suggested that the higher extended basicity ($\text{CaO}+\text{MgO}/(\text{Al}_2\text{O}_3+\text{SiO}_2)$) of a Fe-rich melt is more likely to form glass. Jung and Sohn (2014) studied the crystallisation control of a FeO rich $\text{CaO}-\text{SiO}_2-\text{Al}_2\text{O}_3-\text{MgO}$ slag. The higher basicity of the slag (given by the CaO/SiO_2 ratio) delayed the crystallisation of the molten slag. Esfahani and Barati (2016) investigated the effect of slag composition on the crystallisation of synthetic $\text{CaO}-\text{SiO}_2-\text{Al}_2\text{O}_3-\text{MgO}$ slags. They stated that with an increase in basicity, the CCT and TTT diagrams of the crystallisation shift to the left (shorter time) and higher temperatures. The single-phase inclusions and the matrix of the quasi single-phase inclusions are richer in SiO_2 , Al_2O_3 , CaO, MgO and K_2O than the matrix of the duplex inclusions. These two matrixes are probably a vitreous phase, which did not crystallise during the solidification (Tossavainen *et al.*, 2007; Jung and Sohn, 2014), see Figures 7-a to 7-d. A greater number of Si-O bonds are broken with the increase of basicity, which facilitates the re-ordering of the silicate structure, i.e. faster crystallisation. One of the main differences among the three types of slag inclusions is the FeO content, maximum in quasi single-phase slag inclusions (where the wüstite is the majoritarian phase) and minimum in single-phase slag inclusions (wüstite-free microstructure), see Table 1. The matrix of the duplex slag inclusions is formed by two phases (see Figure 7-c). Fayalite, $2\text{FeO}\cdot\text{SiO}_2$, is the majoritarian phase precipitated in a vitreous matrix. Finally, Na_2O , SO_3 , Cr_2O_3 , and V_2O_5 were not observed in the matrixes of the quasi single-phase and duplex slag inclusions.

Most of the observed oxides are commonly found in many ancient iron artefacts analysed in literature (Buchwald and Wivel, 1998; Dillmann and L'Héritier, 2007; Blakelock *et al.*, 2009; Charlton *et al.*, 2012, Maia *et al.*, 2015; Mamani-Calcina *et al.*, 2017). The chemical analysis of the iron ore available at the Patriótica Iron Factory showed a very pure iron ore containing 98% Fe_2O_3 (Table 1) with 0.6% SiO_2 , 0.4% Al_2O_3 , 0.1% MgO, 0.05% CaO, 0.04% MnO, and 0.03% P_2O_5 . Very few of the world's ironmaking sources could use such pure iron ore. A possible silica source for the slag inclusions is the furnace lining as Horstmann and Toussaint (1989) stated that the lining of the furnaces used local clay - kaolinitic, $\text{Al}_2\text{Si}_2\text{O}_5(\text{OH})_4$. They showed the chemi-

cal analysis of the sponge containing slag and iron (see Table 1), revealing the slag composition. Eschwege (1979) mentioned, "In the construction of small furnaces, coarse grain Itacolomi quartzite, gneiss, soapstone, or even bricks were used." The Itacolomi quartzite, usually employed in the historical monuments in colonial Minas Gerais, contains quartz (SiO_2) and approximately 15% sericite, a type of mica from the muscovite family whose chemical formula is $\text{KAl}_2(\text{Si}_3\text{Al})\text{O}_{10}(\text{OH}, \text{F})_2$ (Neves *et al.*, 2011; Santos *et al.*, 2019). So, the furnace lining may be an essential source of silicon, aluminium and potassium to the slag. Horstmann and Toussaint (1989) attributed the presence of K_2O in the smelting slag to the coal ashes and the Al_2O_3 content to the furnace lining.

Most of the oxides in the slag inclusions are also present in the charcoal ashes (see Table 1), but in a different proportion: CaO, MgO, K_2O , Al_2O_3 , SiO_2 , MnO, and TiO_2 (from the highest to the lowest content) (Dueñas-Gonzales, 2014, Gomes, 2016). The ashes' chemical composition can vary a lot, but they also can explain the presence of all these oxides in the slag of the Patriótica Iron Factory (Sena, 1881). The flux usually used to fluidify the smelting slag might be another source of chemical elements to the slag inclusions (Buchwald and Wivel, 1998; Dillmann and L'Héritier, 2007; Blakelock *et al.*, 2009; Charlton *et al.*, 2012, Maia *et al.*, 2015; Mamani-Calcina *et al.*, 2017). Eschwege (1979) did not mention the addition of fluxes in the furnace load, such as limestone (CaCO_3), to reduce the slag viscosity during the smelting process. However, the use of fluxes was a common practice in the reduction furnaces to facilitate slag removal by simple draining (Blakelock, 2009). In silica-rich slags, usually found in these furnaces, the addition of "basic" (as opposed to acidic) chemical elements, such as calcium and magnesium, reduces the slag viscosity (Blakelock, 2009). The chemical composition of the smelting slag found at the Patriótica Iron Factory (71.4% FeO, 20.9% SiO_2 , 4.1% Al_2O_3 , 1.1% CaO, 1.2% K_2O , 0.23% P_2O_5 and 0.28% TiO_2 , see Table 1) does not show the presence of MgO and MnO (Horstmann and Toussaint, 1989), which were observed in the eyebolt's slag inclusions (see Table 1).

According to Horstmann and Toussaint (1989), the microstructure of the Patriótica's slag showed the presence of wüstite (featuring only Fe peaks in the microanalysis), fayalite (featuring Fe, Si, Ca and Mg), leucite (Si, Al and K) and vitreous (Fe, Si, K, Ca, Fe, P, S and Na) phases. These phases and their proportions were heterogeneously distributed in the slag sample, indicating its substantial chemical heterogeneity. Concerning the appearance of the Patriótica's slag, the authors mentioned, "The slags are apparently furnace slags which have been taken from the furnace together with the iron ball at the end of the reduction process, which is typical for such slags. This is certainly no slag which has flowed out of the furnace during the reduction process in a fully reduced state, but an incompletely reduced slag, which remained in the furnace after the end of the process." Horstmann and Toussaint (1989) did not comment on the low content of CaO in the sponge (~1.0%), which suggests that CaO fluxes were not added to reduce the slag viscosity, which was already standard practice at that time (Blakelock, 2009). The typical content of CaO in viscous slags can vary from 2.5 to 8.6%, for instance, depending on whether it is a tap slag, a bloom slag or a smithing slag (Blakelock, 2009). Eschwege (1812, 1979) confirmed that no fluxes were used in the Patriótica process, "The slag (of The Patriótica Iron Factory) was never completely fluid, remaining in the oven until the end of the operation. It was removed with the bloom".

A mixture of ferritic plates and perlite (the dark region between the plates) is observed close to the eyebolt's surface (bottom of Figure 6-b). In contrast, the eyebolt's interior shows equiaxial grains of ferrite. The pearlite presence indicates that the carbon content near the eyebolt's surface is higher than in the centre (see Figure 6-b). Two intermediate ferrous products from the Patriótica Iron Factory were investigated by Horstmann and Toussaint (1989). They analysed a sponge containing slag and iron, and a bloom. The bloom's chemical analysis revealed 0.6% C, 0.04% P, 0.005% S (indicative of production by charcoal) and 0.02% Mn. The bloom's microstructure was ferritic-pearlitic (with various proportions), indicating that its average

carbon content was between 0.4 and 0.6%. The authors concluded, "This iron (hardenable steel) could be used for the fabrication of agricultural and mining tools which was exactly the aim of Baron von Eschwege". Horstmann and Toussaint (1989) finally correlated the carbon content of the iron bloom produced in Patriótica with the reducing condition of the furnace, "The fact that carburisation has already taken place at such an early stage of reduction proves that strong reducing conditions must have been present". Many ferrous objects have low carbon content regions near the surface since the iron exposure to the oxidising atmospheres at high temperatures decarburises its surface. The eyebolt sample also shows strips of "high" carbon alternately arranged inside the material, demonstrating that this is not a superficial decarburisation effect (see Figure 6-b). The iron bands with the highest carbon content coincide with the regions containing vitreous slag inclusions. In contrast, the iron band with low carbon features large biphasic inclusions. At least three hypotheses can explain the observation of heterogeneous microstructure in the eyebolt concerning the carbon content:

- The "bundled iron" is made by combining iron with different carbon contents, a common technological practice in geographic and historical areas where iron availability is low, encouraging the reuse of various scraps (Colpaert, 1959).

- The carbon gradient is caused by heterogeneous atmospheric conditions inside the furnace since the uneven proportion of charcoal and iron ore can cause localised variations in the atmosphere. In some furnace positions, the atmospheres would more "reducing" (higher CO to CO₂ ratio), reducing the iron oxide to iron and carbonising the metallic iron. In other regions of the furnace, where the atmosphere was more oxidising, the reduction of iron oxide would be incomplete, and the slag inclusions would contain much higher levels of FeO. Consequently, the iron would present low carbon content.

- The microstructural heterogeneity is created by forging. The bloom is pre-forged to expel the excess of liquid slag, and the resulting iron is reheated and forged more intensively. This intense hammering causes more slag expulsion, shaping the iron bloom

into a bar, which is eventually folded and hammered again. The hammering of one part of iron on the other causes both parts to be welded, a process now called "brazing".

There is a similarity between the first and third hypotheses. Still, the analogy with the difference in the chemical composition of the inclusions in the two regions is less clear, as raised by the second hypothesis. Additionally, the existence of thin and continuous layers of iron oxide, see Figure 5-b, suggests malpractice during the forging operation. The presence of these oxidised surfaces indicated no addition of fluxes to promote the fusion of the iron oxide surface and its removal by forging. Light (1987) stated, "one can weld wrought iron, but not mild steel, without flux." Wrought iron is the forged iron with low carbon content, < 0.02% (top of Figure 6-b) and mild steel is the iron-containing 0.1 to 0.2% carbon, therefore having 15 to 30% of pearlite in the microstructure (bottom of Figure 6-b). The literature about the bloom's microstructure produced by the "direct method" (Buchwald and Wivel, 1998; Gordon, 1997) reinforces the association of thermodynamic potential gradient in the furnace's atmosphere with the microstructural heterogeneities of the iron, such as the carbon content and the type of slag inclusion. Gordon (1997) analysed dozens of iron samples and concluded that the slag inclusions of higher carbon regions rarely present high FeO content, and infrequently show wüstite dendrites. Buchwald and Wivel (1998) found similar evidence and discussed the relationship with local variations, in terms of centimetres, in the reducing potential of the furnace's atmosphere. Miller (2002) analysed the microstructure of African archaeological ferrous objects and noted regions with different carbon contents in neighbouring areas of unforged blooms. They also noted layers with varying amounts of pearlite and carbon content in the forged bar. The microstructural characterisation and chemical composition of the slag inclusions of the eyebolt is compatible with the raw materials used by the Patriótica Iron Factory. No discriminating elements could be found either in the eyebolt sample or in the Factory's raw materials that can rule out the possibility that the eyebolt was produced in that ironworks.

4.2. Hammer

The slag inclusions of the hammer present the following phases: wüstite (FeO), magnetite (Fe₃O₄), fayalite (Fe₂SiO₄ with Al₂O₃, K₂O, MgO, CaO and MnO) and vitreous (rich in SiO₂-Al₂O₃-K₂O) (see Figures 10-a and 10-b, and Tables 2 and 3). The P₂O₅ was not identified in the inclusions of the hammer. The slag inclusion amount in the hammer was comparatively lower than the eyebolt (~2.8% vs 4.0% for the eyebolt). The hammer microstructure presented magnetite plates precipitated in the wüstite dendrites, and ferrite halos precipitated at the wüstite/fayalite interfaces (see Figure 10-b and Figure 11). This microstructure indicates that the wüstite (FeO) phase decomposed into ferrite (Fe) and magnetite (Fe₃O₄) at temperatures below 570 °C. The ferrite and magnetite morphologies do not indicate the formation of a lamellar eutectoid structure, where the ferrite grows epitaxially from the Fe₃O₄

surface (Matsuno and Ohmori, 1988). Zhou *et al.* (2012) mentioned that the wüstite eutectoid decomposition promotes the formation of the magnetite/ferrite eutectoid even at cooling rates of about 80°C/s. They also noted that the wüstite decomposition might induce proeutectoid magnetite formation in the wüstite. Sometimes proeutectoid magnetite layer forms at the FeO/steel interfaces. The time-temperature-transformation (TTT) diagrams of the FeO eutectoid decomposition were constructed in dry and wet air conditions, indicating that the rate of isothermal decomposition in wet air was significantly delayed compared to that in dry air (see Figure 12) (Li, 2018).

Considering literature (Matsuno and Ohmori, 1998; Zhou *et al.*, 2012; Li, 2018), the rapid cooling rate during air cooling after forging might produce a nanometric magnetite/ferrite lamellar eutectoid struc-

ture. In this sense, it is not surprising that previous investigators have not yet observed the eutectoid decomposition of the wüstite inside the slag inclusions of ancient ferrous parts (Gordon, 1997; Buchwald and Wivel, 1998; Dillmann and L'Héritier, 2007; Blakelock *et al.*, 2009; Charlton *et al.*, 2012; Maia *et al.*, 2015; Mamani-Calcina *et al.*, 2017). Coarse magnetite plates were present in the wüstite dendrites (preferentially formed at the interface between dendrite and interdendritic region). Additionally, ferrite halos were observed between the primary dendrite and interdendritic region, see Figure 10-b. These results suggest that the hammer service temperature near the surface was below 560°C. However, the service temperature was high enough so that the long thermal-cycling exposure during service allowed the incomplete wüstite decomposition.

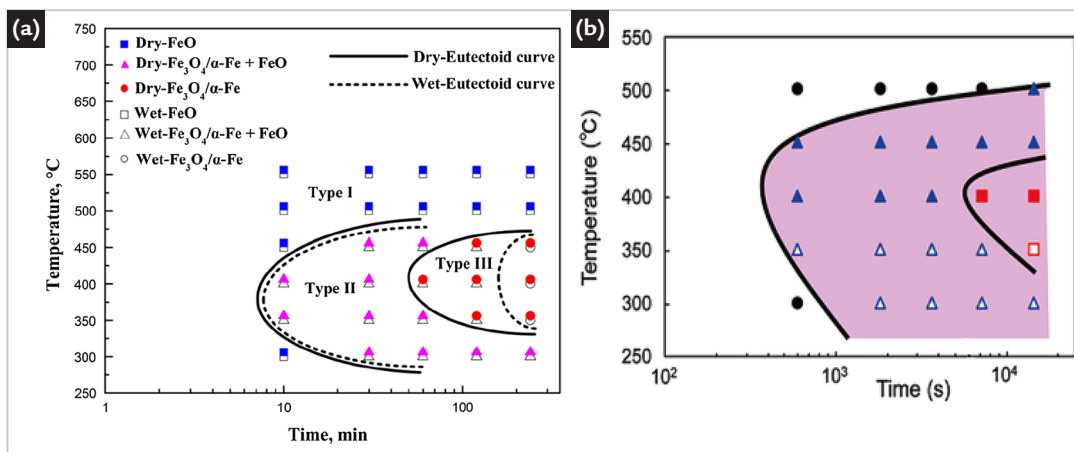


Figure 12 - (a) TTT diagrams of scale thermally grown in dry and wet atmospheres (Li *et al.*, 2018).

In this diagram, the oxide scales can be defined as the following three types: Type I is comprised of the outer Fe₃O₄ layer and inner FeO layer; Type II includes the outer Fe₃O₄ layer, a certain amount of eutectoids, and undecomposed FeO; and Type III consists of the outer Fe₃O₄ layer and the inner eutectoid layer; (b) TTT diagram for magnetite precipitation (Tanei and Kondo, 2016). “▲: Precipitation of Fe₃O₄ from FeO/metal interface, ■: Eutectoid transformation into Fe₃O₄ and ferrite, Δ: Precipitation of granular Fe₃O₄, □: Precipitation of granular Fe₃O₄ and eutectoid transformation.”

Finally, the eyebolt and hammer samples present SiO₂-Al₂O₃-CaO-K₂O rich vitreous phases (see Table 4). The vitreous phase of the hammer presented higher Al₂O₃ (27.5% vs 18.3%) and K₂O (24.2% vs 4.3%) contents than the vitreous single-phase inclusion of the eyebolt. On the other hand, the vitreous single-phase inclusion of the eyebolt presented higher SiO₂ (50.6% vs 38.35), CaO (9.3% vs 2.5%), MgO (6% vs 0%) and MnO (2.8% vs 0%). The analysis of the fayalite phase shows few differences in chemical composition (see Table 4). The hammer's MgO content was higher than the eyebolt's (1.4% vs 0.6%), but the Al₂O₃ content was lower (0.5% vs 4.5%).

Moreover, the eyebolt's fayalite showed 0.8% of K₂O, absent in the hammer's, while the hammer's fayalite showed 0.7% of MnO, absent in the eyebolt's. None of the microconstituents of the hammer's inclusions presented P₂O₅, but P₂O₅ (~1.7%) was observed in the SiO₂-rich matrix of the quasi single-phase eyebolt's inclusions. Consequently, these EDS results indicate that the hammer and the eyebolt were manufactured in different factories. The letter of the governor of Minas Gerais (Baeta, 1973), describing his visit to Patriótica in 1813, suggests the hammer was produced in that Factory. However, it seems unlikely that a 200kg component could be produced

without a hammer with an adequate span. Finally, the chemical composition of the Patriótica Iron Factory slag (Horstmann and Toussaint, 1989) shows the presence of P₂O₅ and peaks of Na and S, which were not found in the hammer inclusions, indicating that the hammer was not produced in the Factory. The characterisation of the microstructure of the slag inclusions and iron allows the construction of reasonable hypotheses about the processing and provenance of metallic artefacts. The archaeometallurgical literature helps complement some historical aspects of the technology, but past facts remain inaccessible in their completeness.

5. Conclusions

5.1 History

• The review on the history of the Patriotic Factory and steel making in Minas Gerais province reinforces the interpreta-

tion that the dozens of forges that operated in this province in late 19th century used a method similar to that implemented by

Eschwege in the Patriótica Iron Factory (low shaft furnaces using water-driven air trompes).

5.2 Eyebolt

• Three different types of slag inclusions were observed in the microstructure of the eyebolt: single-phase microstructure, quasi single-phase microstructure (wüstite and SiO₂-rich matrix) and duplex microstructure (wüstite and SiO₂-rich matrix).

• One of the main differences among the three types of slag inclusions is the FeO content, which is maximum in quasi single-phase slag inclusions (where the wüstite is the majoritarian phase) and minimum in single-phase slag inclusions (wüstite-free microstructure).

• The single-phase inclusions and the matrix of the quasi single-phase inclusions are richer in SiO₂, Al₂O₃, CaO, MgO

and K₂O than the matrix of the duplex inclusions. These two microconstituents are probably a vitreous phase, which did not crystallise during the solidification.

• At higher magnifications, the matrix of the duplex slag inclusions is formed by two phases. The majoritarian phase is the fayalite, 2FeO.SiO₂, precipitated in a vitreous matrix.

• In the metallic matrix of the eyebolt, there is a mixture of ferritic plates and perlite close to the eyebolt's surface. In contrast, the eyebolt's centre shows equiaxial grains of ferrite, indicating that the carbon content near the eyebolt's surface is higher than in the centre.

• There is an inverse relationship be-

tween carbon content in the iron and FeO content in the slag inclusions: the single-phase inclusions are usually surrounded by a ferritic-pearlitic microstructure, while the wüstite-rich inclusions (quasi single-phase and duplex inclusions) by a ferritic microstructure.

• The microstructural characterisation and chemical composition of the slag inclusions of the eyebolt is compatible with the raw materials used by the Patriótica Iron Factory. No discriminating elements could be found either in the eyebolt sample or in the Factory's raw materials that can rule out the possibility that the eyebolt was produced in that Factory.

5.3 Hammer

• Microstructural characterisation of the slag inclusions of the hammer showed an unusual feature: the primary wüstite dendrites suffered partial decomposition into magnetite plates (Fe₃O₄) and ferrite halos (Fe). The ferrite halos were located between the primary wüstite dendrite and the interdendritic region.

• The wüstite decomposition is likely related to the high service temperature at the surface of the forging hammer. The service temperature, however, was thought to be below the eutectoid temperature (~ 560°C).

• The slag inclusion fraction in the hammer was comparatively lower than the eyebolt (~2.8% vs 4.0%).

• None of the microconstituents of the hammer's inclusions presented P₂O₅, but P₂O₅ (~1.7%) was observed in the SiO₂-rich matrix of the quasi single-phase eyebolt's inclusions.

• The eyebolt and hammer samples presented a vitreous SiO₂-Al₂O₃-CaO-K₂O phase. The hammer's K₂O content in the vitreous phase was much higher than the eyebolt's (24% vs 4%), while the hammer's CaO content was lower (2% vs 9%). Additionally, the eyebolt's vitreous phase showed 5.6% of MgO and 2.8% MnO, both absent in the hammer's.

• The eyebolt and hammer samples presented the fayalite phase. The hammer's MgO content in this phase was

higher than the eyebolt's (1.4% vs 0.6%), while the hammer's Al₂O₃ content was lower than the eyebolt's (0.5% vs 4.5%). Additionally, the eyebolt's fayalite showed 0.8% of K₂O, absent in the hammer's, and the hammer's fayalite showed 0.7% of MnO, absent in the eyebolt's.

• The EDS microanalysis results and the volume fraction of slag inclusions indicate that the hammer and the eyebolt were manufactured in different factories.

• The chemical composition of the Patriótica Iron Factory slag shows the presence of P₂O₅ and peaks of Na and S, which were not found in the hammer inclusions, indicating that the hammer was not produced in the Factory.

5.4 General

• The present results help build a database about the characteristics of

early Brazilian iron production products, which creates critical data for future

provenance studies, as it is happening in similar European studies.

Acknowledgements

The authors are grateful to the National Historic and Artistic Heritage Institute (IPHAN), with special mention to Dr J. N. Bittencourt and VALE S.A., a special tribute to Mr W. Delgado. Prof. C. R. F. Azevedo would like to acknowledge the support of the Brazilian

National Council for Scientific and Technological Development (CNPq, grant 310583/2020-9). Prof. F. J. G. Landgraf thanks the support of the CNPq (grant 307631/2018-4), P. E. M. Araújo and R. Schroeder for their criticism and suggestions related to the history of The

Patriótica Iron Factory.

Profs F. J. G. Landgraf, F. Beneduce Neto and C. R. F. Azevedo would like to dedicate this work to the memory of their mentor, the late Professor E. C. O Pinto (1938–2021), metallurgist, researcher and educator.

References

- ÅGREN, M. *Iron-making societies: early industrial development in Sweden and Russia, 1600-1900*. New York: Berghahn Books, 1998. 368 p.
- AGRICOLA, G. *De Re Metallica*. Translated from Latin to English by Herbert Clark Hoover and Lou Henry Hoover. [S. l.: s. n.], 2011. E-book. Available at: <http://www.gutenberg.org/files/38015/38015-h/38015-h.htm>.
- ALFAGALI, C. G. M. *Em casa de ferreiro pior apeiro: os artesãos do ferro em Vila Rica e Mariana no século XVIII*. 2012. 196 f. Dissertação (Mestrado em História) – Instituto de Filosofia e Ciências Humanas, Universidade Estadual de Campinas, Campinas, 2012.
- ARAÚJO, P. E. M. Fábrica de ferro do Morro do Pilar: as três campanhas experimentais e o colapso estrutural do alto-forno na noite de 21 de agosto de 1814. In: SEMINÁRIO NACIONAL DE HISTÓRIA DA CIÊNCIA E DA TECNOLOGIA, 14., 2014, Belo Horizonte. *Anais eletrônicos* [...]. Belo Horizonte: UFMG: SBHC, 2014. 15 p.
- ARAÚJO, P. E. M.; SPORBACK, S. -G.; LANDGRAF, F. J. G. Start-up da siderurgia brasileira. *Revista Metalurgia e Materiais*, São Paulo, v. 66, p. 197-202, 2010.
- ARAÚJO, R. J.; FILGUEIRAS, C. A. L. O Visconde de Barbacena e o químico José Álvares Maciel: encontro na ciência e desencontro na política. *Química Nova*, São Paulo, v. 40, n. 5, p. 602-612, 2017.
- BAETA, N. A. *Indústria siderúrgica em Minas Gerais*. Belo Horizonte: Ed. Imprensa Oficial, 1973. 309 p.
- BLAKELOCK, E.; MARTINÓN-TORRE, M.; VELDHUIJZEN, H. A.; YOUNG, T. Slag inclusions in iron objects and the quest for provenance: an experiment and a case study. *Journal of Archaeological Science*, New York, v. 36, n. 8, p. 1745-57, 2009.
- BUCHWALD, V. F.; WIVEL, H. Slag analysis as a method for the characterisation and provenance of ancient iron objects. *Materials Characterization*, New York, v. 40, n. 2, p. 73-96, 1998.
- CALÓGERAS, J. P. O Ferro: ensaio de história industrial. *Revista do IHGB*, Rio de Janeiro, v. 9, p. 20-100, 1904.
- CHARLTON, M. F.; BLAKELOCK, E.; MARTINÓN-TORRES, M.; YOUNG, T. Investigating the production provenance of iron artefacts with multivariate methods. *Journal of Archaeological Science*, New York, v. 39, n. 7, p. 2280-93, 2012.
- COLPAERT, H. *Metalografia dos produtos siderúrgicos comuns*. 2. ed. São Paulo: Edgar Blücher, 1959. 412 p.
- CUSTODIO, J. Um caso de ferraria proto-industrial: a Chapa Cunha de Mós de Carviçais. In: CUSTÓDIO, J.; CAMPOS, N. (coord.). *Museu do Ferro e da Região de Moncorvo*. Torre de Moncorvo: Museu do Ferro e da Região de Moncorvo, 2002. v.2, p. 187- 219.
- DEZEN-KEMPTER, E. O lugar da indústria no patrimônio cultural. *Revista Labor & Engenho*, Campinas, v. 5, n. 1, p. 107-125, 2011.
- DILLMANN, P.; L'HÉRITIER, M. Slag inclusion analyses for studying ferrous alloys employed in French medieval buildings: supply of materials and diffusion of smelting. *Journal of Archaeological Science*, New York, v. 34, n. 11, p. 1810-1823, 2007.
- DUEÑAS-GONZALES, A. *Caracterização e análise comparativa de cinzas provenientes da queima de biomassa*. 2014. 70 f. Dissertação (Mestrado em Engenharia Mecânica) – Faculdade de Engenharia Mecânica, Universidade Estadual de Campinas, Campinas, 2014.
- DUPRÉ JUNIOR, L. Memória sobre a Fábrica de Ferro de São João do Ipanema. *Anais da Escola de Minas de Ouro Preto*, v. 4, p. 37-68, 1885.
- ESCHWEGE, W. L. *Pluto Brasiliensis*. Tradução Domício de Figueiredo Murta. Belo Horizonte: Itatiaia; São Paulo: Ed. USP, 1979. 306 p. 2v.
- ESCHWEGE, W. L. Memória sobre as dificuldades das fundições e refinações nas fábricas de ferro. *Memórias Económicas da Academia Real das Ciências de Lisboa, Lisboa*, n.4, p. 121-128, 1812.
- ESFAHANI, S; BARATI, M. Effect of slag composition on the crystallisation of synthetic CaO-SiO₂-Al₂O₃-MgO slags: Part I—Crystallisation behaviour. *Journal of Non-Crystalline Solids*, Amsterdam, v. 436, p. 35-43, 2016.
- FELICÍSSIMO JUNIOR, J. *História da siderurgia de São Paulo, seus personagens, seus feitos*. São Paulo: Instituto Geográfico e Geológico. 1969. 153 p.
- FERRAND, P. The iron industry in Brazil (Province of Minas Geraes). *Scientific American*, New York, v. 430, Mach. 1884.
- FERRAND, P. A Indústria do ferro no Brasil. *Anaes da Escola de Minas de Ouro Preto*, v. 4, p. 122-139, 1884.
- FRANÇOIS, J. M. *Recherches sur le gisement et le traitement direct des minerais de fer dans les Pyrénées et particulièrement dans L'Ariege*. Paris: Carilian-Goueuury et V. Dalmont, 1843. 405p.
- FURTADO, J. F. Estudo crítico. In: COUTO, J. V. *Memória sobre a capitania das Minas Gerais: seu território, clima e produções metálicas*. Belo Horizonte: Fundação João Pinheiro, 1994. p. 13-50.
- GOMES, F. M. *História da siderurgia no Brasil*. Belo Horizonte: Itatiaia; São Paulo: EDUSP, 1983. 409 p.
- GOMES, F. P. S. *Valorização de resíduo de cinza de serragem de madeira na produção de piso cerâmico vitrificado*. 2016. 216 f. Dissertação (Mestrado em Engenharia e Ciências dos Materiais) – Universidade Estadual do Norte Fluminense Darcy Ribeiro, Campos dos Goytacazes, 2016.
- GORDON, R. B. Process deduced from ironmaking wastes and artefacts. *Journal of Archaeological Science*, New York, v. 24, n. 1, p. 9-18, 1997.

- HILDEBRAND, K. G. *Fagerstabrukens historia*. Uppsala: Almqvist et Wiksells Boktryckeri, 1957. 487 p. (1, Sexton-och sjuttonhundredatalen).
- HORSTMANN, D.; TOUSSAINT, F. Two Brazilian iron works of the early 19th century Part 2, Metal and slag analyses. *Journal of the Historical Metallurgy Society*, v. 23, n. 2, p. 114-119, 1989.
- INSTITUTO DO PATRIMÔNIO HISTÓRICO E ARTÍSTICO NACIONAL. *Fábrica de Ferro Patriótica*: ruínas (Ouro Preto, MG). [S. l.]: IPHAN, [20--]. Available at: portal.iphan.gov.br/ans.net/tema_consulta.asp?Linha=tc_hist.gif&Cod=1370. Accessed: May 2021.
- JOCKENHÖVEL, A.; WILLMS, C. Archaeological investigations on the beginning of blast furnace-technology in Central Europe. In: CREW, P.; CREW, S. (ed.). *Early ironworking in Europe: archaeology and experiment*. [S. l.]: Plas Tan y Bwlch, 1997. p. 56-58.
- JUNG, S. S.; SOHN, I. Crystallization control for remediation of an FeO-Rich CaO-SiO₂-Al₂O₃-MgO EAF waste slag. *Environmental Science & Technology*, Easton, v. 48, n. 3, p. 1886-1892, 2014.
- LANDGRAF, F. J. G.; ARAÚJO, P. E. M. A arquitetura do alto-forno e a biblioteca perdida de Ipanema: técnica e conhecimento no Brasil Joanino. In: SEMINÁRIO NACIONAL DE HISTÓRIA DA CIÊNCIA E DA TECNOLOGIA, 14., 2014, Belo Horizonte. *Anais eletrônicos* [...]. Belo Horizonte: UFMG: SBHC, 2014.
- LANDGRAF, F. J. G.; TSCHIPTSCHIN, A. P.; GOLDENSTEIN, H. Notas sobre a história da metalurgia no Brasil (1500-1850). In: VARGAS, M. (org.). *História da técnica e da tecnologia no Brasil*. São Paulo: UNESP, 1994. 412 p.
- LI, Z.; CAO, G.; LIN, F.; WANG, H.; LIU, Z. Characterization of oxide scales formed on plain carbon steels in dry and wet atmospheres and their eutectoid transformation from FeO in inert atmosphere. *Oxidation of Metals*, v. 90, p. 337-354, 2018.
- LIBBY, D. C. *Transformação e trabalho em uma economia escravista: Minas Gerais no século XIX*. São Paulo: Brasiliense, 1988. 404 p.
- LIGHT, J. D. Blacksmithing technology and forge construction. *Technology and Culture*, v. 28, n. 3, p. 658-665, 1987.
- MAIA, R. R.; DIAS, M. S.; AZEVEDO, C. R. F.; LANDGRAF, F. J. G. Archaeometry of ferrous artefacts from Luso-Brazilian archaeological sites near Ipanema River, Brazil. *Rem: Revista Escola de Minas*, Ouro Preto, v. 68, n. 2, p. 187-193, 2015.
- MAMANI-CALCINA, E.; LANDGRAF, F. J. G.; AZEVEDO, C. R. F. Investigating the provenance of iron artifacts of the Royal Iron Factory of São João de Ipanema by hierarchical cluster analysis of EDS microanalyses of slag inclusions. *Materials Research*, São Carlos, v. 20, n.1, p. 119-129, 2017.
- MATSUNO, F.; OHMORI, Y. Crystallography of eutectoid decomposition in the FeO oxide layer formed on steel surface. *Transactions of the Japan Institute of Metals*, v. 29, n. 1, p. 8-16, 1988.
- MEDEIROS, L. A Ferraria da Foz do Alge: elemento patrimonial submerso. *Apontamentos de Arqueologia e Patrimônio*, v.4, p. 71-76, 2009.
- MENEZES, R. J. Exposição do governador D. Rodrigo José de Menezes sobre o estado de decadência da capitania de Minas Gerais e meios de remedia-lo. *Revista do Arquivo Público Mineiro*, fasc. II, p. 311-325, 1897.
- MILLER, D. Smelter and Smith: iron age metal fabrication technology in Southern Africa. *Journal of Archaeological Science*, New York, v. 29, n. 10, p. 1083-1131, 2002.
- MILLER, J. R. The direct reduction of iron ore. *Scientific American*, v. 235, n. 1, p. 68-81, 1976.
- NADOLL, P.; MAUK, J. L. Wüstite in a hydrothermal silver-lead-zinc vein, Lucky Friday mine, Coeur d'Alene mining district, U.S.A. *American Mineralogist*, Lancaster, v. 96, p. 261-267, 2011.
- NEVES, J. H.; GODEFROID, L. B., CÂNDIDO, L. C. Avaliação da integridade estrutural do quartzito itacolomi empregado em monumentos históricos de Ouro Preto sem e com colagem usando diferentes resinas. *Rem: Revista Escola de Minas*, Ouro Preto, v. 64, n. 4, 493-498, 2011.
- PENNA, J. A. A Forja catalã de Jean Monlevade e as características de seu produto. *Metalurgia ABM*, São Paulo, v. 31, p. 837-847, 1975.
- PERCY, J. *A treatise on metallurgy, iron and steel*. London: John Murray, Albemarle Street, 1864. 934 p.
- PERCY, J. *Traité complet de métallurgie*. Paris: Librairie Polytechnique Noblet et Baudry, 1865. 632 p. Tome II.
- PINHO, F. A.; NEIVA, I. K. A. *200 anos Fábrica Patriótica: a primeira indústria de ferro do Brasil*. Belo Horizonte: Vale, 2012. 112 p.
- RODRIGUES, A. R. Patrimônio industrial e os órgãos de preservação na cidade de São Paulo. *Revista CPC*, São Paulo, v. 14, p.1-187, 2012.
- ROGERS, E. J. The iron and steel industry in Colonial and Imperial Brazil. *The Americas*, v. 19, n. 2, p. 172-184, 1962.
- SANTOS, A. R.; MENEZES, D. B.; ELLENA, J.; ANDRADE, M. B. Aplicação da espectroscopia Raman na caracterização de minerais pertencentes a uma geocoleção. *Química Nova*, São Paulo, v.42, n. 5, p. 489-496, 2019.
- SCHÖNEWOLF, J. Das "Reisebuch" des Schmelzmeisters Johannes Schönewolf. *Das Werraland*, v.33, p. 36-37, p. 49-51, 1981.
- SCHUBERT, H. R. *History of the British iron and steel industry from c. 450 B.C. to A.D. 1775*. London: Routledge and Kegan Paul, 1957. 445 p.

- SENA, J. C. C. Viagem de estudos metalúrgicos no centro da província de Minas. *Annaes da Escola de Minas de Ouro Preto*, n.1, p. 106-143, 1881.
- SLAG atlas. 2. ed. Dusseldorf: Verlag Stahleisen GmbH, 1995. 663 p.
- SWEDENBORG, E. *Philosophical and mineralogical works*. Dresdae et Lipsiae: Sumptibus Friderici Hekelii, 1734. 386 p. (vol 2, Iron).
- TANEL, H.; KONDO, Y. Phase transformation of oxide scale and its control. *Nippon Steel & Sumitomo Metal Technical Report*, n. 111, p. 87-91, 2016.
- TOMAS, E. The Catalan process for the direct production of malleable iron and its spread to Europe and the Americas. *Contributions to Science*, v. 1, n. 2, p. 225-232, 1999.
- TOSSAVAINEN, M.; ENGSTROM, F.; YANG, Q.; MENAD, N.; LIDSTROM, L. M.; BJORKMAN, B. Characteristics of steel slag under different cooling conditions. *Waste Management*, Amsterdam, v. 27, p. 1335-1344, 2007.
- TOUSSAINT, F. Two Brazilian iron works of the early 19th century. *Journal of the Historical Metallurgy Society*, v. 22, n. 2, p. 73-80, 1988.
- TYLECOTE, R. F. *A history of metallurgy*. London: Institute of Metals, 1984. 205 p.
- VARELA, A. G. Ciência e patronagem na correspondência entre D. Rodrigo de Sousa Coutinho (“Pai e Protetor”) e José Bonifácio de Andrada e Silva (“Venerador Sincero e Criado Humilíssimo”) (1799-1812). In: ENCONTRO DE HISTÓRIA ANPUH, 13., 2008, Rio de Janeiro. *Anais [...]*. Rio de Janeiro: UFRRJ, 2008. 8 p.
- VERGUEIRO, N. P. C. *Memória histórica sobre a fundação da Fábrica de Ferro de São João do Ypanema*. Lisboa: Typografia Rollandiana, 1822. 69 p.
- VIDAL, L.; LUCA, T. R. (org.). *Franceses no Brasil: séculos XIX- XX*. São Paulo: Editora UNESP, 2009. 497 p.
- YIN, J.; HILLERT, M.; BORGSTAM, A. Morphology of proeutectoid ferrite. *Metallurgical Materials Transactions A*, Warrendale, v. 48, p. 1425-1443, 2017.
- ZHOU, C. H.; MA, H. T.; LI, Y.; WANG, L. Eutectoid magnetite in wüstite under conditions of compressive stress and cooling. *Oxidation of Metals*, v. 78, p. 145-152, 2012.

Received: 1 April 2021 - Accepted: 22 June 2021.